

# Spatial Distribution of Non-point Source Pollution in Vembanad Lake

Kichu Paul, Binoy Alias M. & Shiny Varghese  
Department of Civil Engineering  
M.A. College Of Engineering  
Kothamangalam, Kerala

**Abstract**—The Vembanad Lake, the largest backwater system on the southwest coast of India, is subjected to indiscriminate exploitation beyond its supportive capacity. This is a study conducted to assess the status of the non point source pollution distribution of the Vembanad lake using Geographical Information System (GIS). Water qualities, such as acidity, alkanity, Hardness, Chloride, COD, Total Solids, Iron and Sulphate were determined for water samples collected from 35 representative sites of known latitude and longitude for both wet season and dry season. An open source GIS, QGIS, is used to analyse the spatial distribution of these parameters. The analysis indicates Iron, acidity and COD in the wet season and dry season have not undergone significant change. But the values of alkalinity, hardness, chlorine and sulphate have undergone dramatic change. These values have been graphically plotted using GIS interface.

**Keywords**-Vembanad, water quality, GIS (key words)

## I. INTRODUCTION

Kerala has a continuous chain of lagoons or backwaters along its coastal region. These water bodies are fed by rivers and drain into the Lakshadweep Sea through small openings in the sandbars called 'azhi', if permanent or 'pozhi', if temporary. The Vembanad wetland system (Figure1) and its associated drainage basins lie in the humid tropical region between 09°00' -10°40'N and 76°00'-77°30'E. It is unique in terms of physiography, geology, climate, hydrology, land use and flora and fauna. The rivers are generally short, steep, fast flowing and monsoon fed. The Vembanad wetland system includes the Vembanad backwater, the deltaic lower reaches of the rivers draining into it and the adjoining Kol lands. The Vembanad Lake is bordered by Alappuzha (Alleppey), Kottayam and Ernakulam districts of Kerala covering an area of about 200 sq km and extending 80 km in a NW-SE direction from Munambam in the north to Alleppey in the south. The width of the lake varies from 500 m to 4 km and the depth from <1m to 12m. Manimala, Meenachil, Pamba and Achenkovil flow into the lake south of Thanneermukkom and Muvattupuzha river flows into the Cochin backwaters north of Thanneermukkom



Figure 1 Location

Considering the fragile ecosystem of the wetland, deterioration of water quality and consequent damage to aquatic organisms and the shrinkage of Vembanad Lake, this wetland system was included in the National Lake Conservation Programme (NLCP) by the National River Conservation Authority, chaired by the Hon'ble Prime Minister under the Ministry of Environment and Forests (MoEF). Under the NLCP, projects of conservation and management of polluted lakes are taken up on 70:30 cost sharing between the Central and State Governments as in the case of river action plans.

Point source pollution, on the most basic level, is water pollution that comes from a single, discrete place. The term "point source" means any discernible, confined and discrete conveyance, including but not limited to any pipe, ditch, channel, tunnel, conduit, well, discrete fissure, container, rolling stock, concentrated animal feeding operation, or vessel or other floating craft, from which pollutants are or may be discharged. This term does not include agricultural storm water discharges and return flows from irrigated agriculture.

Diffuse water pollution is mainly related to the way we use and manage land and soil. It can affect rivers, lakes, coastal waters and ground waters. Ground waters are vulnerable from, and can be affected by, pollutants that leach from the land surface and from areas of contaminated land. Surface waters are affected by rainfall that washes over and off the land (run-off). Rivers can also be influenced by springs and seepages from groundwater

that contribute to their flow. If the groundwater connection with surface waters is high, pollution can pass from one to affect the other. Run-off has increased as agriculture has intensified and as we have built more roads and houses. This often happens where we have degraded the natural permeability of the landscape and reduced its capacity to retain water.

Unlike point source pollution, we cannot easily control diffuse pollution by issuing licenses or permits. Regulatory approaches have to be more subtle and in many cases need to be well connected to the land use planning system.

## II. STATE OF THE ART

The Vembanad Lake has been subjected to various environmental studies by different agencies. The water quality study conducted by Binu & Harikumar<sup>1</sup> made an assessment on Eutrophication of this lake using Dynamic Model. This study was aiming at point source pollutions. Vincy et.al.<sup>2</sup> conducted a water quality assessment of the Vembanad Lake with reference to backwater tourism. This study indicates the degradation or decline of water quality especially acidity, alkalinity, salinity, hardness, DO etc. Another detailed study conducted by Nazir<sup>3</sup> indicates the degradation of water quality and higher spread of the non source point pollution. Balachandran<sup>4</sup> indicates the progressive deterioration of many of the Indian estuaries including Vembanad Lake caused by anthropogenic activities is of concern because these areas have never been considered as primary targets of conservation. Abhirosh et.al<sup>5</sup> increased prevalence of indicator and pathogenic bacteria in Vembanadu Lake. Prevalence of faecal indicator bacteria, *Escherichia coli* and pathogenic bacteria, *Vibrio cholerae*, *Vibrio parahaemolyticus* and *Salmonella* were analyzed in Vembanadu lake.

The objective of this study was to determine the spatial distribution of the various pollutants across the Vembanad Lake. The scope of the study covers the following

- Identification of the polluted zones in Vembanad lake.
- Policy development to mitigate the pollution due to various sources on the lake.
- Development of strategies for eco restoration.
- Facilitation of the government for maintaining bio diversity of lake.

## III. METHODOLOGY

The Vembanad wetland system and its associated drainage basins lie in the humid tropical region between 09°00' -10°40'N and 76°00'-77°30'E. It is unique in terms of physiography, geology, climate, hydrology, land use and flora and fauna. The rivers are generally short, steep, fast flowing and monsoon fed. The Vembanad wetland system includes the Vembanad backwater, the deltaic lower reaches of the rivers draining into it and the adjoining Kol lands. The Vembanad Lake is bordered by Alappuzha (Alleppey), Kottayam and Ernakulam districts of Kerala covering an area of about 200 sq km and extending 80 km in a NW-SE direction from Munambam in the north to Alleppey in the south.

Analysis of water quality was done both spatially and temporally. 35 representative sites were taken into consideration for a statistically robust analysis. These sites were located between 9° 32' 1.03" N - 76° 22' 2.28" E and 9° 40' 27.99" N - 76° 25' 0.4" E. These sites were chosen taking into consideration the various ecological and human effect that were observed as probable pollution causes, including areas adjacent to resorts and other tourism hotspots; commercial areas such as boat jetties and residential areas such as the R- Block, etc.

The geographical spread of lake can be collected from various sources like toposheets, survey map of India etc. The water samples are collected from the pre-determined sites of the lake. To determine temporal variation the water samples are collected in two seasons, pre monsoon season and post monsoon season.

### WATER QUALITY PARAMETERS

For the analysis of the water sample collected, following tests were conducted according to IS specifications.

1. Acidity
2. Alkalinity
3. Hardness
4. Chloride
5. COD & BOD

6. Total Solids
7. Iron
8. Sulphate

### **Temporal Variation**

The analysis of water quality from the representative sites were done in two seasons, namely, the wet season (Oct-Nov) and the dry season (Jan-Feb). Water quality was checked across 10 parameters, namely, acidity, hardness, alkalinity, sulphates, chlorides, pH, iron, turbidity, solids and COD. These parameters were chosen taking into consideration the type of occupations around the lake and the probable pollution causing agents associated with it. For example, hardness was chosen as a parameter because of the high number of residential and tourism settlements around the lake which discharge untreated soap water into the lake. All the water quality tests were conducted as per Indian Standards.

Another important factor affecting the variation of results in the two seasons was the Thaneermukkam Bund. In the wet season, the bund was open to let flow through to the other side and in the dry season, the bund was closed which reduced the flow of water. Moreover, the level of water in the dry season was very low compared to the wet season.

### **Spatial Variation**

The analysis of water quality was done in 35 representative sites. The above mentioned 10 parameters were analyzed and tests were done similarly as per Indian Standards. The parameters varied with reference to space and this variation can be analyzed with the help of GIS.

### **GIS (Geographic Information System)**

A Geographical Information System (GIS) is a collection of soft-ware that allows you to create, visualize, query and analyze geospatial data. Geospatial data refers to information about the geographic location of an entity. This often involves the use of a geographic coordinate, like a latitude or longitude value. Some typical types of analysis include computing:

1. Distances between geographic locations
2. The amount of area (e.g., square meters) within a certain geographic region
3. What geographic features overlap other features
4. The amount of overlap between features
5. The number of locations within a certain distance of another

The results of analysis may be shown on a map, but are often tabulated into a report to support management decisions.

### **QGIS 1.8.0 (Quantum GIS)**

Quantum GIS (often abbreviated QGIS) is a cross-platform free and open source desktop geographic information systems (GIS) application that provides data viewing, editing and analysis capabilities. It helps to create, edit and export spatial data using digitized tools for vector features, field and raster calculator, georeferencer plug in.

## **IV. FIELD STUDY**

The Vembanad Lake is said to have originated around 5000 years ago during the post glacial era. The lake attained its present configuration around 4th century A.D. The lake supports the livelihoods of a major percentage of the 1.6 million people living in the 38 panchayats around. The most significant eco-system services of Vembanad include support to flood occlusion, fishery, lime shell fishery, agriculture, navigation, port facility and tourism and coir industries. Water pollution from industrial and agro-chemical residues, municipal sewage, effluents from motor boats, and coir retting to open water bodies, etc. deteriorates the quality of the lake ecosystem.

Reconnaissance survey was done on to identify the 35 randomly located critical points (Figure 2). Sample collection for the wet season was conducted. 5 litres of each sample was collected in air-tight containers and shifted to the laboratory within 24 hours. Tests for total acidity, total alkalinity, hardness, chloride, solids, turbidity, sulphate, iron, COD and pH were conducted according to Indian Standard methods.

Vembanad lake is selected for study because large area of water body is being polluted. To find the maximum possible variation in pollutant 35 locations were selected.

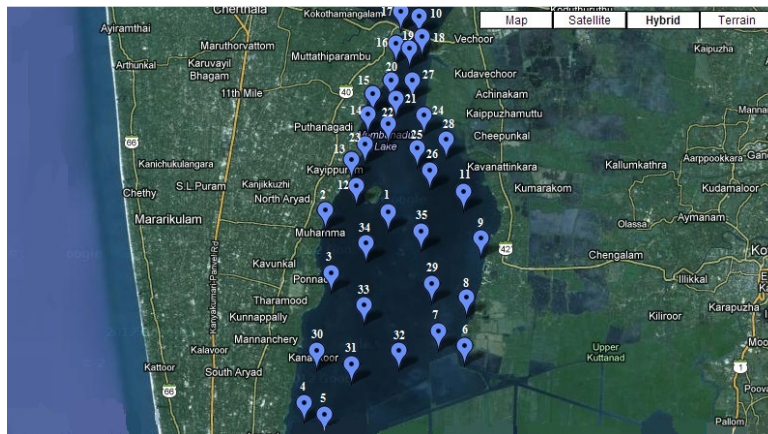


Figure 2 Sampling Sites

## V. RESULT ANALYSIS

The water quality parameters for the 35 sites mentioned above are analysed. The major observations are given below.

**Acidity:** Acidity of water is its quantitative capacity to neutralize a strong base to a designated pH. Strong mineral acids, weak acids such as carbonic and acetic acid and hydrolysing salt such as ferrous or aluminium sulphate contributes to the measured acidity. Figure 3 shows the spatial distribution of acidity. The figure indicates that there is only a slight increase in the value of acidity from wet season to dry season.

**Alkalinity:** The alkalinity of water is its capacity to neutralize acids. Alkalinity of water is a measure of weak acid present in it and of the cations balanced against them. Total alkalinity of water is due to presence of mineral salt present in it. It is primarily caused by the carbonate and bicarbonate ions. Figure 4 shows the spatial distribution of alkalinity. The figure indicates that there is a decrease in the value of alkalinity in dry season compared to that of wet season.

**Chlorides:** Chlorides in the form of  $\text{Cl}^-$  ions is one of the major anions in water. Waters having 250 mg/L chloride may have a salty taste if the cation is sodium. On the other hand, the typical salty taste may be absent even in water containing as much as 1000 mg/L chloride, if the predominant cations are Ca and Mg. As per Indian Standards, the desirable limit of chloride is 250 mg/L. However, the Chloride levels at all 35 stations are below the desirable limit for the wet season. But the values for the dry season are very high.

**COD:** As per Indian standards the COD value of the effluent discharged into the inland waters should not exceed a permissible value of 250mg/l. Figure 6 shows the spatial distribution of COD, and the COD levels at 35 stations are below the desirable limits in both seasons. But for the dry season the COD values are comparatively higher.

**Hardness:** Total hardness is the parameter of water quality used to describe the effect of dissolved minerals (mostly Ca and Mg), determining suitability of water for domestic, industrial and drinking purpose attributed to presence of bicarbonates, sulphates, chloride and nitrates of calcium and magnesium. As per Indian Standards, the desirable limit of hardness for drinking purpose is 300 mg/L. The hardness levels at all 35 stations are below the desirable limits for the wet season. But for the dry season the hardness values are comparatively higher.

**Iron:** As per Indian Standards, the permissible concentration of Fe in portable water is 0.3 mg/L and as per effluent standards the concentration of Iron to discharge into inland surface water is 3 mg/l. The concentration of iron obtained from the 35 stations is low and the values obtained from the two seasons are comparable.

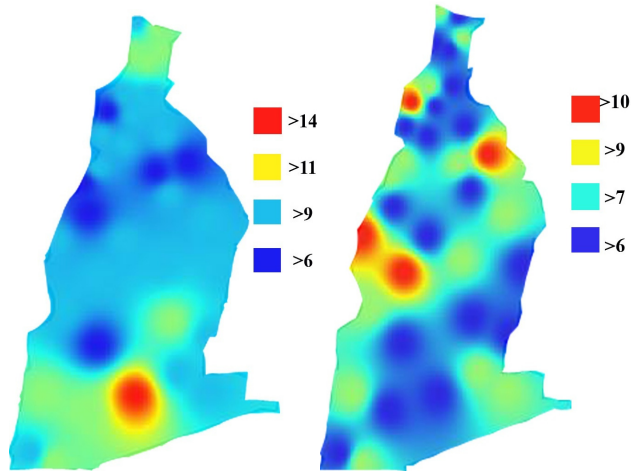


Figure 3 Acidity Wet Season (mg/l)

Figure 3 Acidity Dry Season (mg/l)

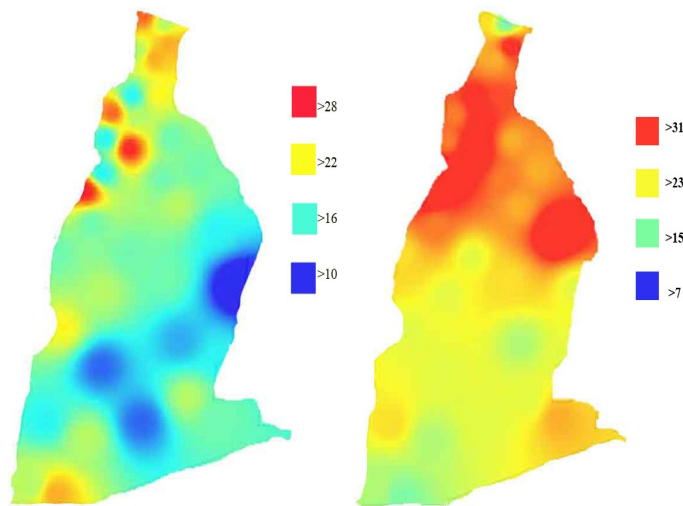


Figure 4 Alkalinity Wet Season (mg/l)

Figure 4 Alkalinity Dry Season (mg/l)

**Sulphate:** According to Indian Standards the permissible limit of sulphate in drinking water is 200 mg/L. The concentration of sulphate for the wet season is low. But the concentration in the dry season is abruptly higher.

**Total solids:** According to Indian Standards the permissible limit of total solids in inland surface water is 2200 mg/L. None of the samples in wet season crossed the permissible limit, but during dry season most of the samples crossed the permissible limit of total solids.

## VI. CONCLUSION

Analysis of water was done from 35 undefined points to assess diffuse pollution characteristics. From the analysis of the results, it can be concluded that the parameters- Iron, acidity and COD in the wet season and dry season have not undergone significant change. But the values of alkalinity, hardness, chlorine and sulphate have undergone dramatic change. These values have been graphically plotted using GIS interface. The variation of the parameters throughout the 35 stations was spatially analyzed.

From the observation of results from dry and wet season, it could be seen that the concentration of parameters was higher in dry season. It was observed that the Thanneermukkam Bund was closed during the dry season and the water depth of the lake was low. Due to this there was no flow of water and this can be a reason for higher

concentrations. Also, the dry season was the tourism season which saw increased number of houseboats on the lake and increased outflow of wastes from these boats and resorts into the lake.

The spatial distribution of the parameters was carried out in the GIS software and the spatial variation of different parameters across the lake and across the two seasons could be analyzed. These analysis results were used for obtaining the relatively higher polluted areas and can help to adopt measures in future.

#### VII. REFERENCES

- [1] Bindu K.R. and Harikumar P.S., Centre for Water Resources Development and Management
- [2] Vincy M.V., Brilliant Rajan and Pradeep Kumar A. P. International Research Journal of Environment Sciences Vol. 1(5), 62-68, December (2012)
- [3] Nasir P. Thesis Calicut university
- [4] K.K Balachandran "Ecosystem modeling of Vembanadu lake"
- [5] Abhirosh Chandran, A. A. M. Hatha and Sherin Varghese "Journal of Water and Health Vol 06 No 4 pp 539-546 "

# A Case Study on Cloud burst induced Landslide

Kichu Paul, Binoy Alias M. & Anniamma Chacko

Department of Civil Engineering  
M.A. College Of Engineering  
Kothamangalam, Kerala

**Abstract—** The devastating landslide which took place at Kadavoor, Kothamangalam on August 17, 2012 shook the lives of many. More than seven families lost their homes and the death toll touched seven in this catastrophic incident. In order to find out the root cause of the landslide, many site visits were conducted and soil samples were collected from 4 different cordon points, with an objective to classify the soil type and determine its cohesion and angle of internal friction. The soil parameters were found out by conducting laboratory tests. Simultaneously, the longitudinal profile of the slope was surveyed and slip circles were plotted for various sections and soil types and minimum factor of safety is determined.

**Keywords-**landslide, cloud bursting, slip circle

## I. INTRODUCTION

Landslides are primarily the result of shear failure along the boundary of moving soil or rock mass. If natural slope fails, it is more probable that failure has been caused by gradual decrease of shear strength than by extreme condition at the time of failure. Presence of water increases the weight of the soil mass and leads to the reduction in shear strength. Hence water has been implicated as the main controlling factor in most of the slides. Studies conducted in the state have revealed that prolonged and intensive rainfall resulting in pore water pressure variations are the most important trigger for landslides. The process leading to landslide was accelerated by anthropogenic disturbances such as deforestation and cultivation of crops lacking capability to add to root cohesion in steep slopes.

Some other alternative mechanisms can be invoked to explain the phenomenon. For instance, the mechanism of gradual “smoothing” of the sliding surface was proposed by Kokusho (not for the Kadavoor landslide). He supposed that when a soil layer of significant thickness underneath the sliding surface liquefies, and the soil directly on top is of low permeability (both conditions might also apply to the Kadavoor landslide), then the natural tendency of the liquefied layer to settle could produce a very slim “film” of water, only a few centimeters or even millimeters in thickness. The development of this water film along the sliding surface could explain the extent of the runoff (about 100 m). Figure 1 shows the site at Kadavoor where the land slide occurred.



Figure 1 Site at Kadavoor

## II. LITERATURE REVIEW

It is generally recognized that rainfall induced landslides are caused by increased pore pressures and seepage forces during the periods of intense rainfall (Terzaghi 1950; Sidle and Swanston 1982; Sitar et al.1992; Anderson and Sitar 1995). It is the increased pore pressure that decreases the effective stress in the soil and thus reduces the soil shear strength eventually resulting in slope failure (Brand 1981; Brenner et al. 1985). Further studies have illustrated that in some cases of rainfall induced landslides movement along the sliding surface leads to crushing of soil grains, which results in liquefaction along its surface finally resulting in rapid movement and long run out distance (Sassa 1996; Sassa 1998a, b); thus high pore pressure is the result of shearing along the sliding surface. Liquefaction, a process by which soil suddenly loses a large proportion of its shear resistance due to the generation of high pore pressure is a reason for fluidised landslide. Liquefaction triggered by dynamic effects , such as earthquakes or by static effects such as rainfall, snowmelt has been studied extensively (Eg: Terzaghi 1956; Seed 1966 , 1979; Bishop 1967,1973; Castro 1969, Casagrande 1971; Castro and paulose 1977; Sassa

1984,1996,1998a,1998b; Eckersley 1985,1986; Hird and Hassona 1990, Ishihara et al 1990) and much knowledge has been accumulated about mechanism of liquefaction.

The major objective of the study is to identify the root cause of the landslide by assessing the soil type and determining the shear strength parameters. The factor of safety is determined by Swedish Circle method. The stability of the existing slope is judged there by.

### III. METHODOLOGY

Soil sample was taken from 4 cordon points Figure 2. The fourth sample was taken at a point located in the top right corner of the slope which hadn't slide off due to the landslide. The soil samples were classified after conducting wet sieve analysis. Important soil parameters like cohesion and angle of internal friction was found out from direct shear test. The longitudinal profile of the slope was obtained after conducting survey.

Longitudinal section was taken in 7 directions and slip circles were drawn. Each circle was divided into 5 slices. Several slip circles were plotted changing the values of cohesion and angle of internal friction. The factor of safety (It is the ratio of available shear strength to that required to keep the slope stable) for each case was found out and it can be assumed that the landslide conformed to the soil parameters which gave the minimum factor of safety. Swedish circle method was adopted for finding the factor of safety. In this method, the sliding mass above the failure surface is divided into a no of slices. The force acting on each slice is obtained by considering the mechanical equilibrium of the slices.



Figure 2 Site spots for sampling

### IV. OBSERVATION AND ANALYSIS

After conducting wet sieve analysis, sample 1, 2, 3 and 4 were reported as sandy type soil. The cohesion and angle of internal friction were determined as per the specification. The Factor of Safety for all the 7 sections were determined. A plot of factor of safety on all sections is given in Figure 3

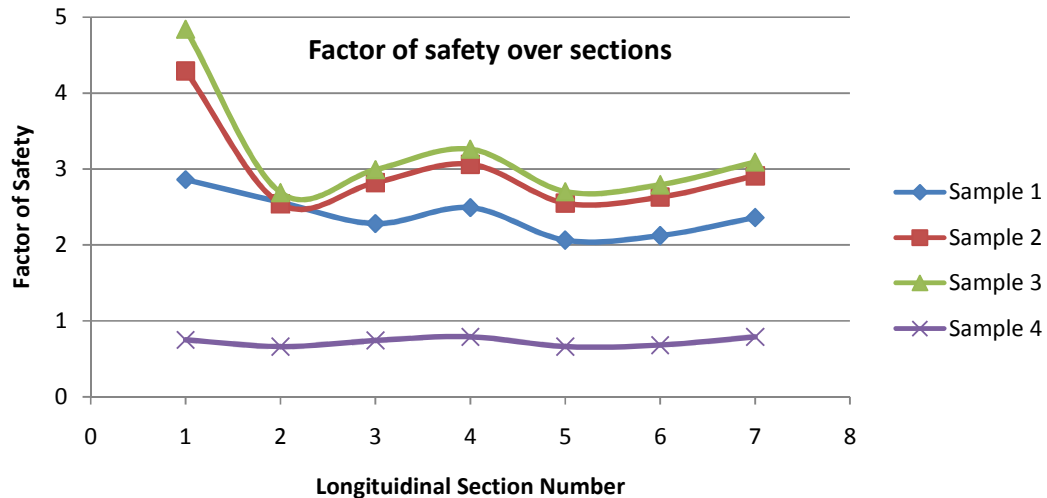


Figure 3 Factor of Safety on different Sections

It can be clearly seen that in each of the 7 sections taken, factor of safety falls below 1 if occupied by soil sample 4. All the other soil specimens gave a value of factor of safety higher than 1 which indicates stability of the slope. Hence it can be concluded that soil specimen 4 was responsible for the landslide trigger along with other several possibilities. It can also be suggested that after the heavy rain the pore water pressure at the slip surface increased, reducing the effective normal stress and thus diminishing the restraining friction along the slip line. This is combined with increased soil weight due to added groundwater. A shrinkage crack at the top of the slip would have also filled with rain water, pushing the slip forward.

## V. CONCLUSION

From the factor of safety calculations it can be inferred that soil type 4(sandy soil) might be responsible for triggering the slide. Since saturated conditions existed at the top of the slope before the occurrence of the landslide, the increased unit weight of the soil also might have contributed to the slide. The combination of soil and topographic amplification could have played a major role in triggering the landslide. In such a case, the basic free field motion could have possibly been amplified within the sliding mass. With such an excitation, the developing shear stresses could possibly lead to liquefaction of even marginally sensitive soil layers which would have resulted in a catastrophe of this magnitude.

## VI. REFERENCES

- [1] Sassa K, Fukuoka H, Scarascia-Mugnozza G, Evans S. Earthquake induced landslides: distribution, motion and mechanisms. *Soils Found* 1996;53–64 [special issue].
- [2] Kallou P, Gazetas G. *Dynamic analysis of Nikawa landslide*. In: Proceedings of the fourth Hellenic conference on geotechnical and geoenvironmental engineering, vol. 2, Athens, 2001. p. 171–8.
- [3] Kokusho T. Mechanisms for water film generation and lateral flow in liquefied sand layer. *Soils Found* 2000;40(5):99–111.
- [4] Sassa K. Development of a new cyclic loading ring shear apparatus to study earthquake-induced-landslides. Report for grant-in-aid for development of scientific research by the
- [5] Sassa K, Fukuoka H, Evans S, Scarascia-Mugnozza G, Furuya G, Vanikoff D, et al. A rapid landslide in Nikawa disasters, Bangkok, 1980. Investigation research on the 1995 Hyogoken-Nambu earthquake and its damages. 1995. p. 244–58 [in Japanese].
- [6] Anderson DL. An earthquake induced heat mechanism to explain the loss of strength of large rock and earth slides. In: Proceedings of the international conference on engineering for protection from natural Nishinomiya city triggered by the Hyogoken-Nambu earthquake. Report of scientific grant-in-aid for scientific research (project no. 06306022, Representative: T. Fujiwara).
- [7] Voight B, Faust C. Frictional heat and strength loss in some rapid landslides. *Geotechnique* 1982;32(1):43\_54.
- [8] Vardoulakis I. Catastrophic landslides due to frictional heating of the failure plane. *Mech Cohesive-Frict Mater* 2000;5:443\_67.
- [9] Vardoulakis I. Thermo-poro-mechanical analysis of rapid fault deformation. In: Proceedings of the fourth international conference on micromechanics of granular media, Sendai. Balkema: Rotterdam; 2001. p. 273–80.

# Derivation of Secondary Electron Energy Spectrum at Different Atmospheric Depth

Rena Majumdar  
Department of Physics  
Bhairab Ganguly College  
Kolkata-56, India  
rksahabkp@gmail.com

**Abstract—** The all particle primary nucleon spectrum has been estimated on the basis of the latest PAMELA, CREAM, ATIC-2 BALLOON BORNE EXPERIMENTAL DATA. The concept of nuclear fragmentation has been used to estimate the nucleon flux from nuclei spectra. Using this spectra, we have calculated analytically the energy spectra of the secondary electrons originated from the decay of charged and neutral pions initiated on the upper atmosphere from the primary nucleon-air collision in the energy (4-1000) GeV. The calculations are valid up to an atmospheric depth of about (3.8-7.4) gm-cm<sup>-2</sup>. The derived results are compared with the experimental electron fluxes available from Boezio et al., Torri et al., Aguilar et al. Chang et al. and Yoshida et al. using PPB-BETS detector.

## I. INTRODUCTION

The investigation on primary cosmic rays is necessary in the study of cosmic ray acceleration and propagation through the atmosphere and also in testing the validity of models in high energy interactions with the interstellar matter. The secondary component electron is the lowest mass constituents of the cosmic rays. In contrast to heavier cosmic rays, acceleration and propagation process for electrons are affected by synchrotron energy loss and inverse Compton scattering. Consequently, electron flux observations can be compared with other cosmic ray measurement to yield insight into cosmic ray acceleration and propagation process. It has been recognized that the spectra of electrons give us unique information about the propagation acceleration of cosmic rays in ISM. Muller et al. [1] have suggested that the containment volume of electrons includes regions beyond the disk of the galaxy, the spectrum at the acceleration site has a power law exponent 2.65 and the time scale of containment in the galaxy is independent of the energy of the electrons. They have used radio data from the galactic anti-center direction for analysis. Mauger et al. [2] have shown a truncated path-length distribution due to lack of nearby sources could be responsible for the additional steepening of the electron spectrum. Van der Walt [3] has investigated the validity of the Thomson limit for inverse Compton scattering up to electron energies of 1000 GeV. Nishimura et al. [4] have estimated the possible contribution of nearby sources to the high energy electrons.

Ptuskin and Ormes [5] have discussed the anisotropy of very high-energy electrons based on the diffusion from local SNRs. They have given an extremely high anisotropy amplitude. However, it is not easy to obtain the electron spectrum in the high energy region above 1TeV, because we need a rejection power of more than 10<sup>4</sup> against protons, which exceeds the limit of current emulsion technology with microscopes. To solve the problem, Yoshida et al. [6] have observed the cosmic ray electrons in the energy range 10 GeV to 1 TeV at the top of the atmosphere with the PPB-BETS detector consisting of 36 scintillating fiber belts, 9 plastic scintillation counters, and 14 lead plates with a total thickness of 9 radiation lengths. The basic structure is similar to that of BETS detector of Torri et al. [7], but several improvements have been adopted to observe high energy electrons. Recently Chang et al. [8] have achieved the electron observations in the energy region from 20 GeV to 1TeV using ATIC-2 balloon experiment.

In the present work, the flux of secondary electrons has been derived from the decay of charged and neutral pions initiated by primary p-air collisions in the energy range 10 to 1000 GeV at different atmospheric - depth 3.8 , 5.6 and 7.4 gm- cm<sup>-2</sup> . The derived result has been compared with experimental data of Boezio et al. [9], Torri et al. Aguilar et al. [10], Chang et al. and Yoshida et al

## II. NUCLEAR PHYSICS AND KINEMATICS

Bhadhwar et al. [11] have modified the formulation of e-energy spectrum obtained from charged  $\pi$  meson decays which obeys the formula.

$$J_{e^{-}}(E)dE_p = \frac{2(\gamma+6)}{(\gamma+1)(\gamma+3)(\gamma+4)} \left(\frac{m_p}{m_\pi}\right) \frac{Am}{m_p} \int_R^\infty \frac{d\sigma_{\pi^{-}}(E, E_p)}{dE} E_p^{-(\gamma+4)} dE_p \quad (1)$$

where  $AE_p^{-(\gamma+4)}$  is the all particle primary nucleon spectrum with the spectral amplitude A and integral index  $\gamma$ ; m is the matter traversed by primary nucleons in air;  $m_p = 1.67 \times 10^{-24}$  gm is the proton mass in gm,  $m_\mu = 0.10566$  GeV,  $m_\pi = 0.13957$  GeV are the rest energies of muon and pion respectively;  $\frac{d\sigma_{\pi^{-}}}{dE}$  is the invariant cross section taken from the fit to the accelerator data of the  $pp \rightarrow \pi^{-}X$  inclusive reaction. Verma [12] has given the e-spectrum obtained from neutral  $\pi$  meson.

$$J(E, m) = \frac{4F(E_\pi)}{\Lambda_i \Lambda_\gamma} m^2 \left[ 1 - \frac{m(\Lambda_p + \Lambda_\gamma)}{3\Lambda_p \Lambda_\gamma} \right] \quad (2)$$

where

$$F(E_\pi) = \frac{1}{2} (Z_{p\pi^+} + Z_{p\pi^-}) AE_p^{-(\gamma+4)} \quad (3)$$

is the production spectrum of charged  $\pi^-$  meson,  $\Lambda_i$  is the interaction mean free path of protons,  $\Lambda_\gamma$  is the characteristic length for pair production, m is atmospheric depth,  $\Lambda_p$  is the absorption mean free path of proton in air in gm-cm<sup>-2</sup>.

### III. RESULT AND DISCUSSION

Several balloon and satellite borne active and passive detector experiments on the determination of primary cosmic nuclei fluxes viz., H, He, C, N, O, Ne, Mg, Si, and Fe have been performed by PAMALLA collaboration [13], CREAM [14], ATIC-2 [15], HEAO [16] and are displayed in Figs. 1-8.

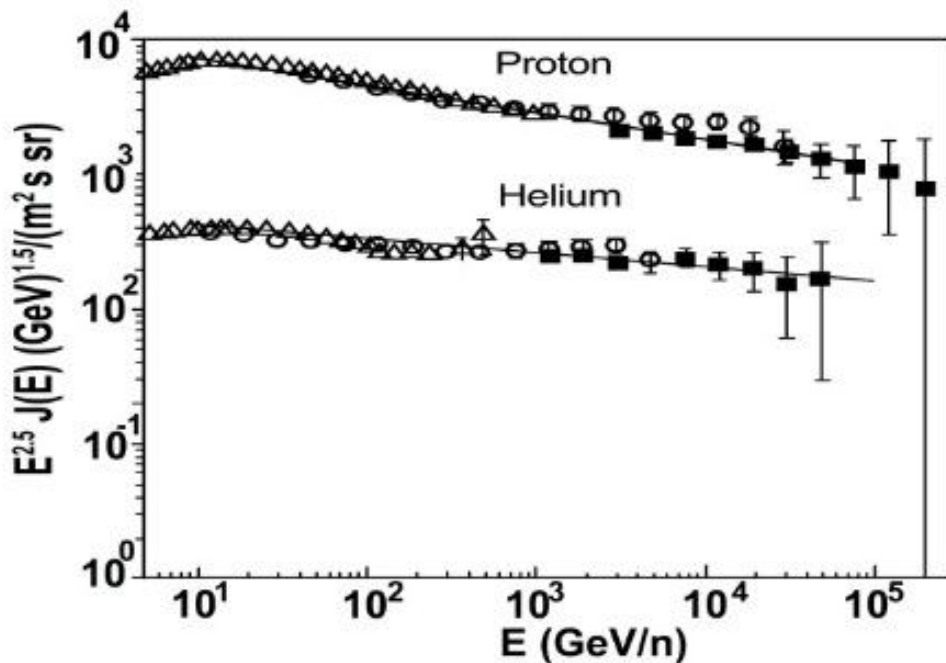


FIGURE 1 :  
 △ : PAMELLA – 2013  
 ■ : CREAM – 2011  
 ○ : ATIC2 – 2009  
 — : PRESENT WORK (FITTED)

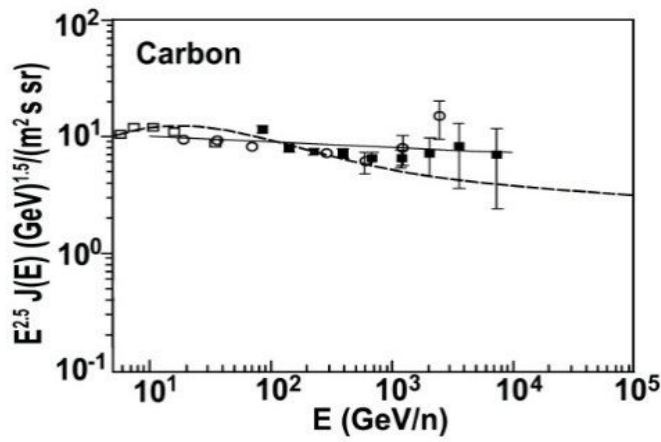


Fig.2

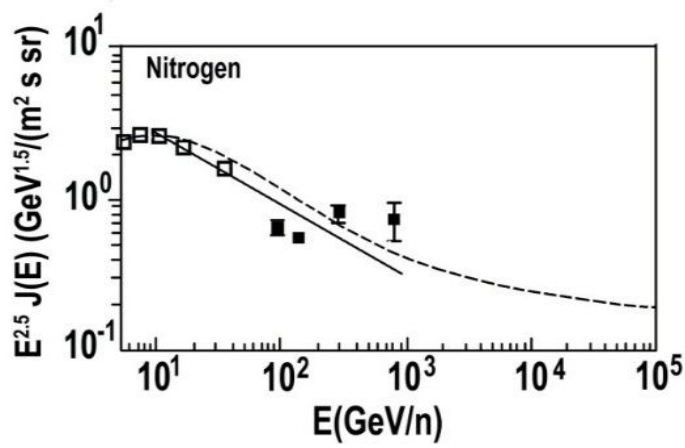


Fig.3

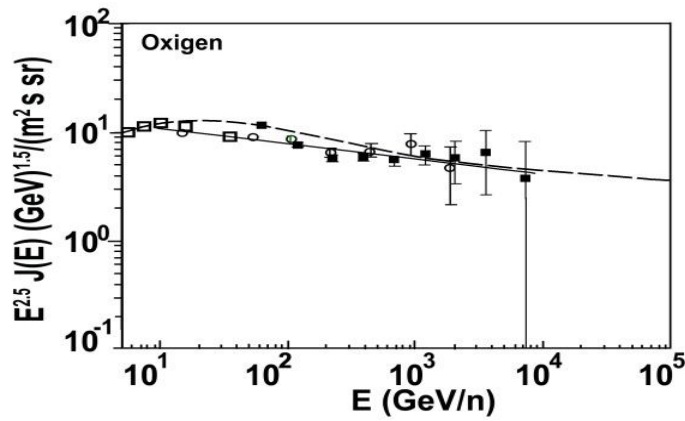


Fig.4

○ : HEAO - 1990      ■ : CREAM - 2011  
□ : ATIC2 - 2009

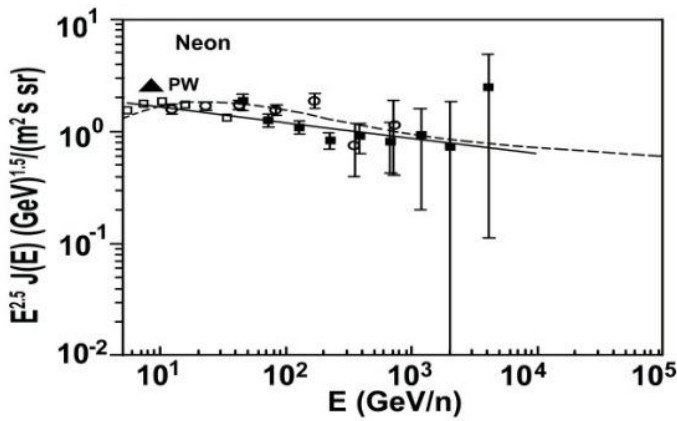


Fig.5

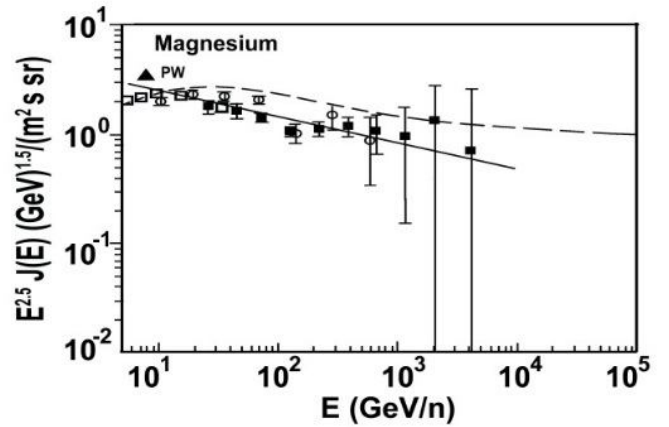


Fig.6

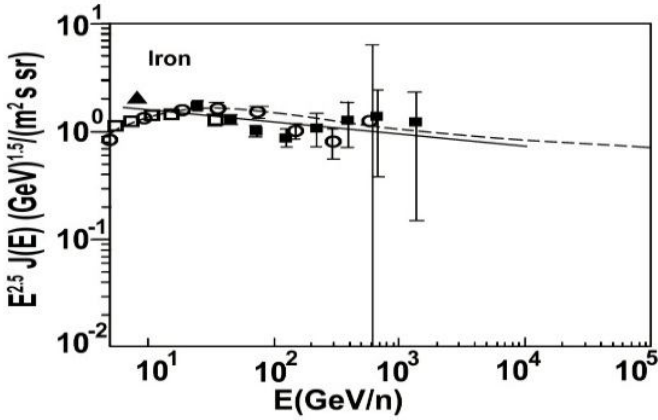


Fig.7

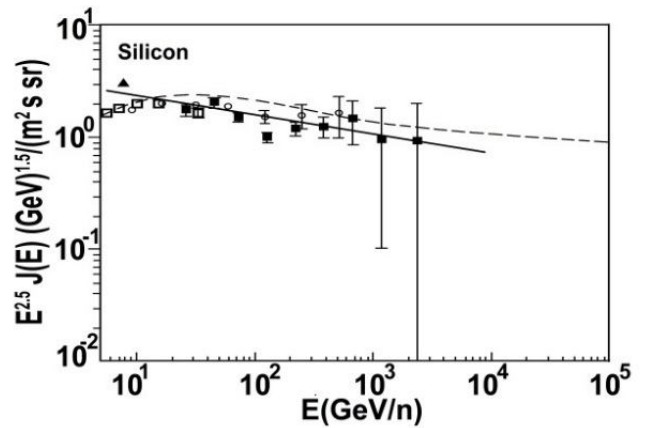


Fig.8

○ : HEAO - 1990      ■ : CREAM - 2011  
 □ : ATIC2 - 2009      ▲ : PW (1995)  
 — : PRESENT WORK (FITTED)

The fit to these data are exhibited in those plots and follows the power law form for energy range between  $10-10^4$  GeV and the parametric values are shown in Table-1.

TABLE-1

Element (i)	Mass number(A <sub>i</sub> )	Differential spectral amplitudes K <sub>i</sub> in (cm <sup>2</sup> sec sr GeV/n) <sup>-1</sup>	Spectral Index (γ)
P	1	1.24	2.71
He	4	5.25×10 <sup>-2</sup>	2.61
C	12	9.6 ×10 <sup>-4</sup>	2.53
N	14	8.18×10 <sup>-4</sup>	2.96
O	16	1.52×10 <sup>-3</sup>	2.64
Ne	20	2.1×10 <sup>-4</sup>	2.56
Mg	24	4.3×10 <sup>-4</sup>	2.73
Si	28	3.356×10 <sup>-4</sup>	2.66
Fe	56	2.05×10 <sup>-4</sup>	2.61

The latest all particle primary nucleon spectrum in the energy range EP = (10-10<sup>4</sup>) GeV has been found to follow the form

$$J_{p+n} = 1.53 E^{-2.7} dE \quad (4)$$

The CERN ISR data on the pp → π<sup>-</sup> X inclusive reaction cross-section can be fitted by the power law

$$\left(x \frac{d\sigma}{dx}\right)_{\pi^-} = 23.3963 (1-x)^{5.02mb} \quad (5)$$

for 0.1 < x < 0.6.

The flux of electrons originated from the decay of charged π<sup>-</sup> meson at different depths have been estimated from the relation (1) in the energy range (4-10<sup>2</sup>) GeV and follows the power law

$$J_{e^-} = K(m) E^{-2.7} (m^2 \text{ s. sr. GeV})^{-1} \quad (6)$$

for K(m) = 4.79, 7.06, 9.33 (for m = 3.8, 5.6, 7.4 gm-cm-2 respectively).

Table-2 shows the parametric values of interaction mean free path of protons (Λ<sub>1</sub>), the absorption length of protons in air (Λ<sub>p</sub>), the characteristic length of protons for pair production (Λ<sub>γ</sub>) in gm – cm<sup>-2</sup> air, fractional energy moments in p-air collision for π<sup>-</sup> and π<sup>+</sup> productions, Z<sub>pπ<sup>-</sup></sub> and Z<sub>pπ<sup>+</sup></sub> respectively.

The estimated parametric values of Λ<sub>1</sub>, Λ<sub>p</sub>, Λ<sub>γ</sub> in g-cm<sup>-2</sup> air and Z- factors are displayed in table 2.

Λ <sub>1</sub>	Λ <sub>p</sub>	Λ <sub>γ</sub>	Z <sub>pπ<sup>+</sup></sub>	Z <sub>pπ<sup>-</sup></sub>
70	110	38	0.04099	0.0283

The estimated Z- factors [17] for p-p collision have been corrected for p-air collision by adopting the conventional procedure of DAR [18]. The Z factors provide a good measure of the shape of the inclusive reaction cross-section which gives an estimate of the primary energy flow to secondaries generated in air showers.

Using these parametric values, the fluxes of electrons obtained from neutral π meson can be estimated from (2) at different atmospheric depths and the corresponding power law becomes

$$J_{e^-} = T(m) E^{-2.7} (m^2 \text{ s. sr. GeV})^{-1} \quad (7)$$

for  $T(m) = 23.38, 32.28, 45.54$  for  $m = 3.8, 5.6, 7.4 \text{ gm-cm}^{-2}$  respectively.

In the present investigation we have adopted the scaling hypothesis of Feynman[19] for the estimation of meson spectrum initiated by p-p collision in the upper atmosphere. The scaling hypothesis is assumed to be valid at relativistic energies above 6 GeV. So the minimum threshold of electron energy should be above 4 GeV which is free from Albedo electrons [20,21]. Therefore the derived electron spectrum has been compared with data measured above 4 GeV.

Now the total secondary electron spectrum is obtained by accounting the contributions from the sum of (1) and (2) and is plotted in Fig.9.

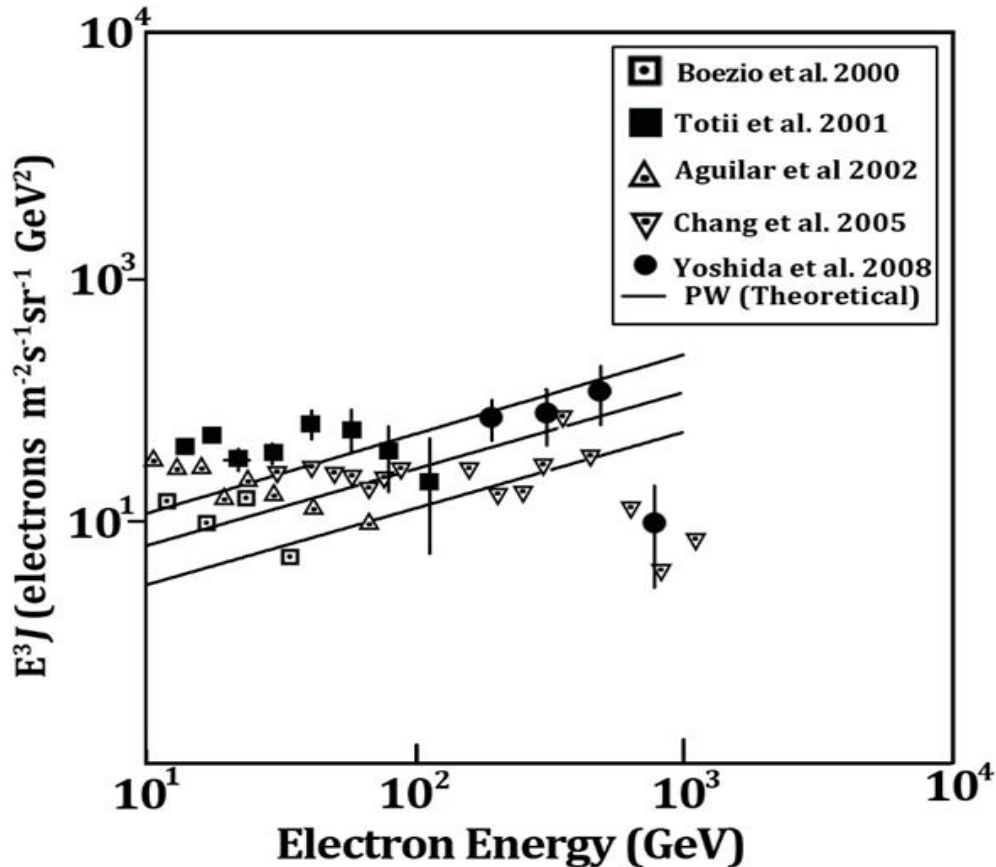


Fig-9

#### IV. CONCLUSIONS

Using the latest primary nucleon spectrum and CERN differential cross section data, the energy spectra of cosmic ray secondary electron spectra at different atmospheric depths (3.8 – 7.4)g/cm<sup>2</sup> have been calculated. The derived spectra have been found comparable with experimental data of Boezio et al., Torii et al., Aguilar et al., Chang et al. and Yoshida et al.

#### REFERENCES

- [1] D.Muller and J.Tang: in Proc.18th ICRC, Bangalore, vol-2, 1983, p-60.
- [2] B. G. Mauger and J. F. Ormes: in Proc. 18th ICRC, Bangalore, vol-2, 1983, p-65.
- [3] Van der Walt: in Proc. 22nd ICRC, Dublin, vol-2, 1991, p-141.
- [4] J. Nishimura, T.K. obayashi et al.: in Proc. 25th ICRC, Durban, vol-4, 1997, p-233.
- [5] V.S. Ptuskin and J. F. Ormes: in Proc. 24th ICRC, Rome, vol-3, 1995, p-56.

- [6] K. Yoshida, S. Torri et al., *Advances in Space Research*, 42, 2008, 1670.
- [7] S. Torri , T. Tamura et al. , *Nucl. Instrum. Methods Phys.ResA*, 452, 2000, 81.
- [8] J. Chang, W.K.H, et al. in *Proc. 29th ICRC, Pune, vol-3, 2005, p-1.*
- [9] M. Boezio, P. Carlson et al. *Astrophys. J.*, 532, 2000, 653.
- [10] M. Aguilar, J. Alcaraz et al. *Phys.Rep.*, 366, 2002, 331.
- [11] G. D. Badhwar, R. L. Golden et al., *Astrophys. Space Sci.*, 37, 283, 1975.
- [12] S. D. Verma: *Proc. Ind. Acad. Sci.*, 66, 1967,125.
- [13] PAMELLA collaboration, O. Adriani et al., *Science*, 332, 2011, 69.
- [14] Y. Yoon et al., *Astrophys. J.*,728, 2011, 122.
- [15] A. Panov et al., *Bull. Russ. Acad. Sci. Phys.*, 73, 2009, 564.
- [16] J. Engelmann, P. Ferrando et al., *Astron. Astrophys.* 23, 1990, 96.
- [17] O. C. Alkofer, D. P. Bhattacharyya and P. Pal, *IL NuovoCimento*, 9C, 1986, no. 2, 421.

# FEASIBILITY STUDY OF ARECA REINFORCED CONCRETE

Lovely K.M, Jithesh K, Laju Kottalil, Jaleen George  
Department of Civil Engineering,  
Mar Athanasius College of Engineering  
Kothamangalam ,Kerala, India

**Abstract— The construction using areca as reinforcement in concrete is one method to reduce cost of construction. In this work feasibility of concrete using areca as reinforcement instead of steel in concrete was studied.**

**Keywords-:** *Areca Concrete, Steel, Flexural Strength, Cement*

## I. INTRODUCTION

The elegant and beautiful areca tree belongs to the family of 'Palmae'. The areca tree can rise up to 18 or even 30 m. It has a girth of only 45 cm. It bears a crown of long, feathery leaves at the summit of its slender, branchless stem. The slim grey coloured stem is ridged with the scars of fallen leaves and crowned by a polished area of green or orange colour. The wood of the tree can be used to make bows and spear handles and the trunk forms a good staging pole. The main advantage of areca tree is that the arecas are available in plenty in India. It is one of the main cultivations in some states in India. It gives arecnuts for 25 years to farmers. After 25 years fruit yielding capacity will decrease. After that the tree will be cut off and new one will be planted. Areca can grow in any climate. A single areca tree can produce approximately 45 numbers of 20 m long ,10 mm dia areca strips which is equivalent to 558 kg steel. It is a very flexible plant that sways in the wind and is cheaper also. Tests have proven that areca is a viable alternative for steel.

## II. MATERIALS

The properties of cement, fine aggregate and coarse aggregate were studied. The tests were done at the concrete laboratory

### *A Tests on Cement*

Tests were conducted to find the physical properties of cement as per BIS and the values are presented in Table 1.

**Table 1. Test results of Cement**

Property	Results	
Make	Penne	
Specific Gravity	3.15	
Normal Consistency	31 %	
Fineness	4%	
Initial Setting time	150 min	
Final setting time	360 min	
Soundness	2 mm	
Compressive strength	3 <sup>rd</sup> day	18 MPa
	7 <sup>th</sup> day	25 MPa
	28 <sup>th</sup> day	36MPa

*B Tests on Fine Aggregate*

Clean river sand free from dirt, twings etc. and passing through 4.75 mm sieve was used as fine aggregate. Tests were conducted as per Indian Standards. Properties of fine aggregate are given in Table 2 and Table 3.

**Table 2. Sieve analysis of fine aggregate**

IS Sieve Designation	4.75mm	2.36 mm	1.18 mm	600 micron	300 micron	150 micron	pan
Weight retained(g)	7	9	751	50	158	20	5

**Table 3 Properties of fine aggregate**

Property	Results	
Specific Gravity	2.57	
Water absorption	1 %	
Organic impurities	Nil	
Bulk density	Loose	1.42 kg/l
	Compact	1.48 kg/l

*C. Tests on Coarse Aggregate*

Crushed gravel of 20 mm down size was used as coarse aggregate. The Aggregate conforming to IS: 383-1970 was used. Properties of coarse aggregate were found out as per BIS and are presented in Tables 4 and Table 5.

**Table 4. Sieve analysis of coarse aggregate**

IS Sieve Designation	40 mm	20 mm	10 mm	4.75 mm	2.36 mm
Weight retained(g)	100	267	722	11	0

**Table 5 Properties of Coarse aggregate**

Property	Results	
Specific Gravity	2.65	
Water absorption	0.57	
Organic impurities	Nil	
Bulk density	Loose	1.46 kg/l
	Compact	1.54 kg/l

**III MIX DESIGN**

All concrete samples were prepared using designed mix. Mix design for M 20 and M 25 grade concrete were done based on BIS Method of Mix design. The quantities of cement, fine sand, coarse sand and water was

measured by weight. . Test specimens were of size 15 cm x 15 cm x 15 cm. After 24 hours the specimens were marked and removed from moulds and kept in a tank for curing until taken out just prior to test. Three cubes from each grade of concrete mix were prepared and tested as per IS :516 at 3 days, 7 days and 28 days. The test results are shown in Table 6.

**Table 6. Concrete mix Details**

Mix	Ratio	Quantity in kg			Water/ cement ratio	Compressive strength (MPa)		
		Cement	Fine aggregate	Coarse aggregate		3 <sup>rd</sup> day	7 <sup>th</sup> day	28 <sup>th</sup> day
M 20	1;1.6:3.47	50	80	173.5	0.54	11	18	26
	1;63:3.57	50	81.5	178.5	0.58	8	14	20
	1;1.57:3.39	50	78.5	169.5	0.58	12	20	28
M 25	1:1.26:2.49	50	63	124.5	0.40	16	21	28
	1:1.29:3	50	64.5	150	0.49	14	18	25
	1:1.24:2.89	50	62	144.5	0.49	19	23	29

#### IV. EXPERIMENTAL STUDIES

Testing plays an important role in adopting the areca as reinforcement in concrete. Simple, direct and convenient methods were applied to find strength of the reinforcement and concrete. Method of tests for strength of concrete were done as per IS: 516. Sampling and analysis of concrete were done as per IS: 1199. The following factors were considered in the selection of areca tree for use as reinforcement in concrete structures.

1. Twenty five year old areca trees were used for the test
2. Seasoned areca was used
3. Avoided green colour tree
4. Only bottom two third portion of tree was used

##### A Sizing

The tree was split into splints 8 mm dia, 8 mm square, 10 mm dia, 10 mm, square, 12 mm dia, 12 mm square, 14 mm dia, 14 mm square, 16 mm dia, 16 mm square, 20 mm dia, 20 mm square. The splitting was done at saw mill.

##### B Modulus of Elasticity

Modulus of Elasticity of areca  $E_a$  was determined as per IS :1708-1986. The test results are given in Table 7

**Table 7. Test results of Modulus of Elasticity**

Properties	Results
Diameter	10.6 mm
Area	88.247 mm <sup>2</sup>
Gauge length	26.5 mm
Initial length	200 mm
Final length	206 mm

*C Tensile strength of Areca reinforcement*

According to the procedure for testing areca, a specimen tested without supports is bound to slip out of the testing machine. It is therefore advised to make wooden supports for the specimen to provide better grip. The specimen was glued to the wood supports using ‘carpenters’ wood glue. Ten areca trees are cut off and allowed to dry for one month. The tree was supported at regular intervals. The tree was split into splints 8 mm dia, 8 mm square, 10 mm dia, 10 mm square, 12 mm dia, 12 mm square, 14 mm dia, 14 mm square, 16 mm dia, 16 mm square, 20 mm dia, 20 mm square. The splitting was done at saw mill. The mechanical property of areca reinforcement is shown in Table 8.

**Table 8 Mechanical property areca reinforcement**

<b>Mechanical property</b>	<b>Value</b>
Ultimate tensile strength	256 N/mm <sup>2</sup>
Minimum tensile strength	63 N/mm <sup>2</sup>
Maximum tensile strength	42 N/mm <sup>2</sup>
Modulus of Elasticity	26680 N/mm <sup>2</sup>

*D Tensile strength of Steel reinforcement*

Tensile strength of steel was determined to compare the results of areca and steel. Peekay make steel bars were used. The results are given in Table 9.

**Table 9. Tensile strength of Steel reinforcement**

<b>Material</b>	<b>Test results (N/mm<sup>2</sup>)</b>				
	<b>6 mm</b>	<b>8mm</b>	<b>10 mm</b>	<b>12 mm</b>	<b>16 mm</b>
MS bar	260	265	270	265	270
FE 415 bar	430	435	440	439	445

*E Testing of Concrete samples*

The samples were tested and the flexural strength was determined. The average flexural strength of beams of plain concrete and areca reinforced are given in Table 10.

**Table 10. Flexural strength of beams**

Sl. No.	Specimen	Average flexural strength ( N/mm <sup>2</sup> )		
		3 <sup>rd</sup> day	7 <sup>th</sup> day	28 <sup>th</sup> day
1	Plain Concrete	2.36	3.61	5.42
2	Areca reinforced with 2 nos. 6 mm square	2.72	4.31	5.84
3	Areca reinforced with 2 nos. 6 mm dia.	2.77	4.63	5.89
4	Areca reinforced with 2 nos. 8 mm square	2.9	4.76	6.15
5	Areca reinforced with 2 nos. 8 mm dia.	2.93	5.00	6.66
6	Areca reinforced with 2 nos.10 mm square	3.52	5.65	7.11
7	Areca reinforced with 2 nos. 10 mm dia.	3.45	5.78	7.4
8	Areca reinforced with 2 nos. 12 mm square	3.56	5.78	7.61
9	Areca reinforced with 2 nos.12 mm dia.	3.72	6.2	8.06
10	Areca reinforced with 2 nos.16 mm square	3.84	6.2	8.81
11	Areca reinforced with 2 nos. 16 mm dia.	3.77	7.35	9.44
12	Areca reinforced with 2 nos. 20 mm square	3.42	6.17	8.53
13	Steel reinforced with 2 nos. 6 mm dia. Fe 415	5.02	7.72	9.13
14	Steel reinforced with 2 nos. 8 mm dia. Fe 415	7.45	9.21	9.83
15	Steel reinforced with 2 nos. 10 mm dia. Fe 415.	9.13	11.57	13.86
16	Steel reinforced with 2 nos. 12 mm dia. Fe 415	10.36	11.38	14.07

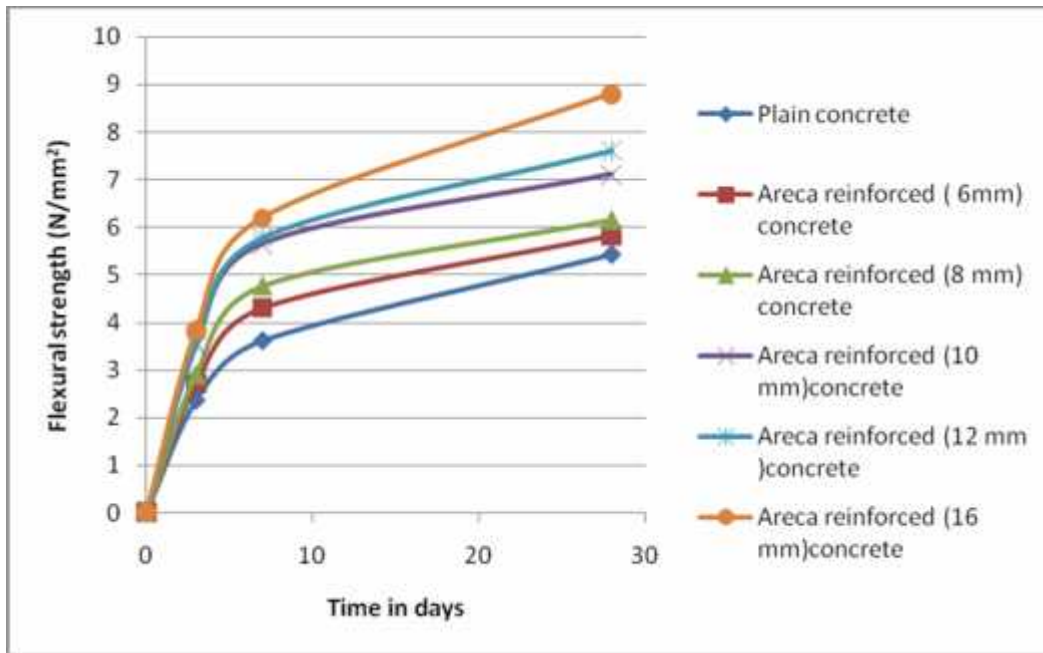
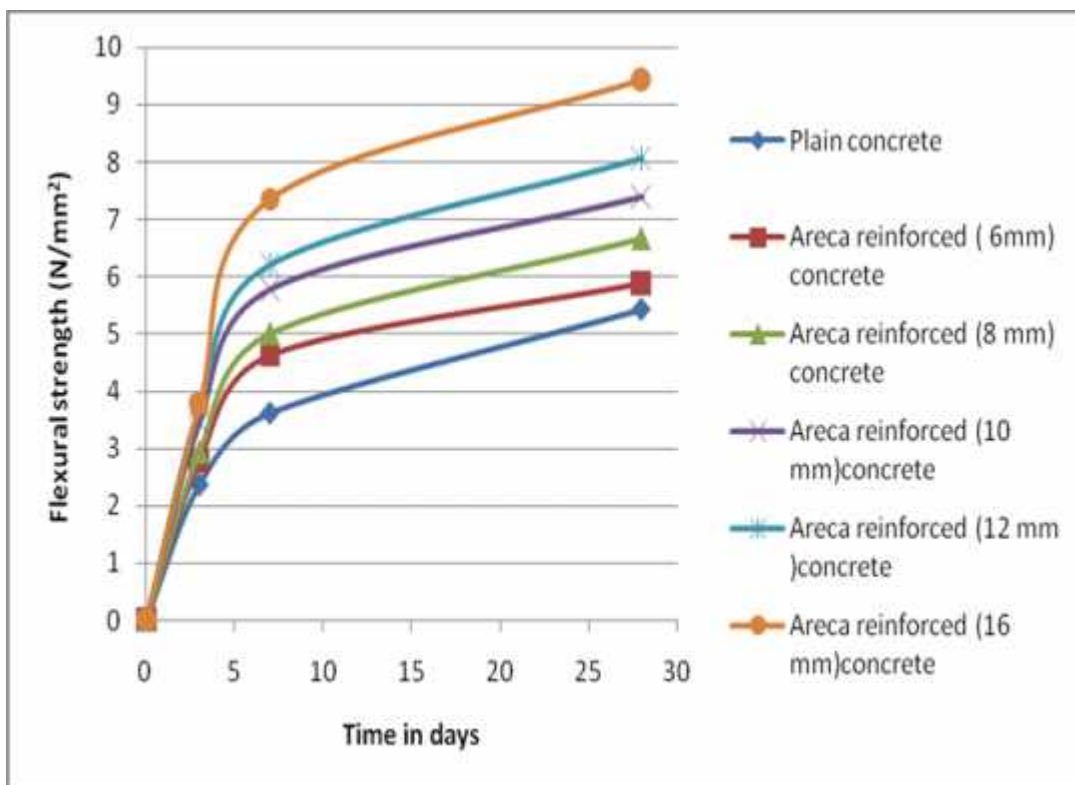


Fig. 1 Relationship between time and flexural strength of Concrete using square shaped areca



**Fig. 2 Relationship between time and flexural strength of Concrete using round shaped areca**

**V RESULTS AND DISCUSSIONS**

The mechanical and physical properties of areca were determined. Areca gives tensile strength up to 256 N / mm<sup>2</sup>. Minimum tensile strength was 63 N / mm<sup>2</sup>. When the flexural test was conducted , the concrete beam reinforced with areca has taken load more than that of plain concrete even though it shows improper bonding in concrete. It shows that, if the proper bonding was done the result would be improved. Flexural strength of beams and slabs of plain, areca reinforced and steel reinforced beams were determined.

**VI CONCLUSION**

A comparative study of the areca and steel bars and comparative study of flexural strength of plain concrete,, areca reinforced and steel reinforced concrete were studied..The salient conclusions from the study are summarized below.

1. The results of the investigations show that the areca can substitute steel satisfactorily
2. Application of areca can be considered as a low- cost construction material.
3. Areca might not be a good alternative for high span slabs.
4. Water proofing coating is recommended to increase its bonding when areca is used as reinforcement.
5. Further studies regarding bond strength and durability are required before complete confidence of using areca as reinforcement.

**REFERENCES**

- [1] P. Baruah and S. Talukdar, “ A comparative study of compressive , flexural, tensile and shear strength of concrete with fibres of different origins “,The Indian Concrete Journal, Published by ACC Limited, Vol.81,p 23, July 2007.
- [2] Journal, “Workshop on Advances in Cement and Concrete Technology”, Indian Institute of Bridge Engineers, Secendarabad,1995
- [3] Khosrow Ghavami,” *Bamboo as reinforcement in Structural Concrete elements* ”,Cement and Concrete Composites 27,p 637-647,2005.
- [4] IS: 456-2000, “ *Indian Standard Code of Practice for plain and reinforced concrete*”, Bureau of Indian Standards, New Delhi,2002.
- [5] M. L. Gambir, “ *Concrete Technology* ,” Tata McGraw Hill Publishing Company limited, New Delhi, 2005.

# USER AUTHENTICATION BY SECURED GRAPHICAL PASSWORD IMPLEMENTATION

Anil H. Rokade\*, Zafar Ul Hasan\*\*, Sonali A. Mahajan\*\*\*

Hi-Tech Institute of Technology, Aurangabad, India, email: mr.anil2097@rediffmail.com\*

Sandip Foundation, Nashik, India, email: zafarulhasan@rediffmail.com\*\*

Govt. Engg College, Aurangabad, India, email: mahajansonali8@gmail.com\*\*\*

**Abstract**— Graphical password is very strong password as compare to the text password and which is easily we can remember. Those who are use this system, authenticate themselves by identifying correct images fro set of displayed images. However, despite the impressive results of user studies on experimental graphical passwords schemes, their overall commercial adaptations have been relatively less. In this paper, we have searched reasons behind the less commercial acceptance of graphical password and we have invent such technique to overcome the limitation of existing system. Based on this technique we design graphical password Main goal of this system is to work as a cued recognition based graphical authentication scheme that allows users to make combination of text , images and numbers as their password, we have the strengths of Numbers, Alphabets and Pictures together to effectively defeat prevalent forms of social hacking. We have taken sample test of a user study with 65 participants to evaluate the viability of our proposed design. Results of the test are very good which indicates that our proposed systems early starting is secure.

**Keywords-** authentication, Graphical User passwords, Usable security, high probability.

## I. INTRODUCTION

User authentication is a major problem in every system providing secure access to confidential information and personalized services. Although, today there exists numerous ways to authenticate a person [1, 2], the most popular method amongst them is with passwords. In this knowledge based authentication scheme, user authenticates herself by presenting the knowledge of a secret string of alphanumeric characters. The secret string is called as *password* and it is assumed to be known only to the claimed identity and hence her identity gets verified. However, in practice, anyone who knows or guesses the password is also able to authenticate as the legitimate user. Passwords represent simple, cost effective and user friendly authentication solution since its usage requires no special hardware or training and passwords can be easily distributed, maintained and updated via telephone, fax or email. However, passwords are effective only if following two conflicting requirements are satisfied simultaneously [3].

- **Usability:** Passwords should be easy to remember and user authentication process should easy for humans and should take less time.
- **Security:** Passwords should be secure; that is, they should look random and should be hard to guess; they should be changed frequently and should be different on different accounts of the same user; they should not be written or stored down in plain text. remembered for a longer time, better than the text. An illustrative example is shown in Figure 1.



Figure 1: What is easy to remember, a picture of *Golden Temple* or a set of numbers?

As we can see in Figure 1, the task of memorizing a list of ten random digits, after a few seconds of inspection, would be impossible for most of us. On the other hand, the aerial picture of *Golden Temple* could easily be memorized so that at some future time, it could be distinguished from variety of other scenes.

The fact that images are better remembered than text and can potentially be chosen from an infinite set of images makes graphical passwords an ideal replacement to text passwords, especially in environments where the text entry is awkward or limited (For example, mobile phones, Point of sale (POS) devices and ATMs) . Even though the area of graphical passwords is actively discussed in the academic arena and experimental graphical password schemes [3,6, 7] present promising results in terms of improved memorability, overall commercial adaptations of graphical passwords has been low.

The aim of this paper is to investigate the reasons behind low commercial acceptance and provide suitable recommendations to overcome them. In the second half of this paper, based on these recommendations, we design a simple graphical password scheme, called USER AUTHENTICATION BY SECURED GRAPHICAL PASSWORD IMPLEMENTATION. USER AUTHENTICATION BY SECURED GRAPHICAL PASSWORD IMPLEMENTATION is a cued recognition based graphical authentication scheme, which allows users to choose both text as well as images as passwords without any specific alternations to underlying authentication design and process. It also blends together the strengths of Numbers, Alphabets and Pictures (NAP) to effectively defeat prevalent forms of social hacking. In this paper we describe the complete design of USER AUTHENTICATION BY SECURED GRAPHICAL PASSWORD IMPLEMENTATION and argue for its potential benefits in terms of security and usability. We then provide results of user study and security analysis. Finally, we conclude with the summary of our contribution.

## 2. RETHINKING GRAPHICAL PASSWORDS DESIGN

When graphical passwords were first introduced, it was conceived that the picture superiority effect coupled with the large password space offered by images, would solve the password problem entirely (the conflict between the security and usability) and people would choose graphical passwords that are stronger than the text passwords they typically select. However, in practice, results were not as expected. Graphical passwords have issues in both usability and security [ 13, 14] Balancing them together is as difficult as it was in text passwords. As a result, even after a lot of academic attention and recommendations, graphical passwords are rarely used in practice.

In this section, we review some of the common problems associated with graphical passwords. Our focus is mainly on Co geometric graphical password schemes.

### 2.1 Usability Issues

Security experts often say that users are the weakest link in a security system [1, 7]. Users misunderstand how to use security mechanisms and do not realize the need for such a protection. User behavior is essentially goal driven and security is usually a supportive task. Users are happy to circumvent the security measures, if security measures try to impede their primary tasks. It is imperative therefore to consider carefully the usability of the proposed authentication scheme. As explained earlier, authentication process should take less time, it should be easy and stress free for the users. However, graphical passwords present some problems in terms of the efficiency (time to execute) and affordance.

### 2.2 Security

Compared to text passwords, graphical passwords are weak against some of the common attacks on passwords schemes. We list down some of the common attacks and how related proposals have tried to mitigate them.

### *2.2.1 Brute force and dictionary based attack*

Simplest of the attack against any authentication scheme is to randomly guess the correct password. For example, an attacker needs 10,000 attempts to correctly guess a four digit Personal Identification Number PIN. Dictionary attack is more sophisticated attack than brute force. Here, instead of random guessing, attacker tries to crack the password using a dictionary of most common passwords.

## *3. LITURATURE SURVEY*

Existing literature and experience in graphical passwords design have led us to following observations that laid the foundation for this work.

### *3.1 Personal vs. Random images*

The success of the graphical password scheme strongly depends on the type of images used [12]. For example, user can create a portfolio using personal images or random images. Both approaches have advantages and disadvantages. Psychological results show that self-generated or personal images are better recognized than those that are not [25]. However, such images are insecure in practical setting due to their vulnerability against guessing attacks. System-chosen random images on the other hand, are more secure against guessing attacks, but they are difficult to remember than personal images [8, 9, 36]. Ideally, we desire an authentication scheme that can merge together the security benefits of system-chosen images and memorability gains of self-chosen images.

### *3.2 Cognitive flexibility*

We must realize that cognitive flexibility is important to accommodate people with different cognitive ability [13]. For users who do not want the visual way of working or prefer the traditional text passwords, graphical passwords should inhabit some alternate mechanism that allows them to select and enter text passwords.

### *3.3 Selection of decoy images*

As we said earlier, locating password images involves visual search which consumes time. In order to improve the efficiency, the selection of decoy images becomes crucial, in a sense that these images should be both visually and semantically distinct so that users are not confused while locating their password images.

### *3.4 Cued Recognition*

A cued recognition is an interesting approach to graphical passwords design. In such schemes, a cue is given to the user that helps her in the recognition of portfolio images. Best example of such a scheme is a Story scheme [16], where the story or the semantic relationship between the images assists user in the recognition of chosen password images. However, the cue should be designed carefully so that it only helps the legitimate user and not the attacker.

## *4. USER AUTHENTICATION BY SECURED GRAPHICAL PASSWORD IMPLEMENTATION: OUR PROPOSED SCHEME*

USER AUTHENTICATION BY SECURED GRAPHICAL PASSWORD IMPLEMENTATION is a novel co geometric graphical authentication scheme which involves recognition of portfolio images. During account setup user creates a portfolio of 4 images or 4 characters or a 4-character word as her password and recognizes the images that corresponds to the chosen password to login. Motivation behind USER AUTHENTICATION



#### 4.3 Usability features of

##### USER AUTHENTICATION BY SECURED GRAPHICAL PASSWORD IMPLEMENTATION

USER AUTHENTICATION BY SECURED GRAPHICAL PASSWORD IMPLEMENTATION is a simple graphical password scheme, easy for users to grasp, but at the same time, it provides good levels of security to keep fraudsters at bay. The main usability features are listed below.

- **Improved memorability:** In the image set, we have specifically chosen images of the very first objects that come to mind when we think of the letter associated with it. For example, A for Apple, B for Ball etc. These images are very easy to remember and recall.
- **Cognitive scalability:** Our proposed scheme is language independent. Use of pictures and symbols makes the scheme ideal for use by the people of all abilities and age with any level of literacy. It also provides both textual and pictorial support to accommodate people with different cognitive abilities.
- **Simple, cost effective and stress free login experience:** Our proposed scheme achieves the desired security without the aid of any extra hardware or token. USER AUTHENTICATION BY SECURED GRAPHICAL PASSWORD IMPLEMENTATION also do not need costly software installations or dedicated hardware to run. The login interface is intuitive and specially designed, keeping the cognitive abilities of the users in mind.
- **Software as a Service (SaaS):** USER AUTHENTICATION BY SECURED GRAPHICAL PASSWORD IMPLEMENTATION can easily be integrated into current secure online authentication architecture and can replace passwords or serve as a second form of authentication. It is compatible (Adaptive) across various financial domains and transaction types like ATM, ecommerce, and mobile commerce.
- **Configurable:** Various attributes of USER AUTHENTICATION BY SECURED GRAPHICAL PASSWORD IMPLEMENTATION (number of images, length of the password etc) can be customized to increase security and to meet the specific needs of the customer.
- **Advertising opportunities:** Industries can leverage the opportunities to advertise on the USER AUTHENTICATION BY SECURED GRAPHICAL PASSWORD IMPLEMENTATION by allowing their images inside USER AUTHENTICATION BY SECURED GRAPHICAL PASSWORD IMPLEMENTATION. The ad images can be tailored to meet the needs of the user demographic.

##### 5. SECURITY OF USER AUTHENTICATION BY SECURED GRAPHICAL PASSWORD IMPLEMENTATION

We recommend that USER AUTHENTICATION BY SECURED GRAPHICAL PASSWORD IMPLEMENTATION, should be implemented and deployed in systems where offline attacks are not possible and where number of guess attempts are limited per account in a given time period (For example, ATMs). We assume that all communication between the user and the server is made secure through SSL, thereby avoiding simple attacks based on network sniffing. Below, we enlist countermeasures against possible attacks on USER AUTHENTICATION BY SECURED GRAPHICAL PASSWORD IMPLEMENTATION.

#### 5.1 Brute force attack

To crack USER AUTHENTICATION BY SECURED GRAPHICAL PASSWORD IMPLEMENTATION password, attacker must guess the four password images from 5x5 grid. However, in USER AUTHENTICATION BY SECURED GRAPHICAL PASSWORD IMPLEMENTATION, there are 3,03,600 (25P4) possible patterns of selecting four images out of 25 images. Alternatively an attacker can try to randomly guess the one time access code. The access code is a combination of four digits (each digit can be any number between 0 - 9). Therefore, the total number of valid combination of one time access code is 10,000, if the ordering constraint is kept. Without the ordering constraint, the number of possible valid combinations reduces by a factor of 4! Furthermore, limiting the login attempts can strengthen security of USER AUTHENTICATION BY SECURED GRAPHICAL PASSWORD IMPLEMENTATION.

## 5.2 Dictionary attack

In USER AUTHENTICATION BY SECURED GRAPHICAL PASSWORD IMPLEMENTATION, each user authenticates herself with a set of four random images. She can either choose these images directly or use them as a cue for her text password of four letters. Users are free to use dictionary words as password. Although this may appear as a threat since an attacker can build a dictionary of most common four-letter words, we wanted to note that, according to scribble [17], there exist around 3,957 possible four-letter English words (excluding names of person, places and abbreviations). Therefore, building such dictionary may not be economical if we guard the number of successive login attempts.

## 5.3 Social engineering attack

We employ Probabilistic one time password strategy [18] described earlier to defeat prevalent forms of identity theft through social engineering. Explaining the theory behind the Probabilistic one time password strategy is beyond the scope of this paper. Interested readers can refer to the work of Bedworth [18] and Brostoff et al. [19].

At every login, images are randomly placed in the grid with a different set of numbers associated with them. With every login, the positions of images as well as the associated numbers within the grid change, making the password unique per session. Further, the position of images in the grid is irrelevant to the authentication process. Thus identity theft using following social engineering techniques is difficult.

### 5.3.1 Resistance against Shoulder surfing:

User never actually selects her true password images, by clicking on it. So anyone who is piping over the shoulder or even with hidden cameras can only be able to see the one time access code, which changes with each login session. Thus should ensuring is not effective.

### 5.3.2 Protection against malware attacks:

Our proposed scheme can be made effective even without the keyboard, therefore no advantage with key loggers. Even if someone captures and records the screen, she will still not be able to deduce your password as every time grid pattern is randomly generated and the password that is formed with given pattern is used only once.

## 6. USER STUDY OF USER AUTHENTICATION BY SECURED GRAPHICAL PASSWORD IMPLEMENTATION

One aspect of our user study aimed to test the usability of USER AUTHENTICATION BY SECURED GRAPHICAL PASSWORD IMPLEMENTATION. Is it simple? Is it easy to understand and convenient to use? Another goal of our user study was to learn the characteristics of user-chosen passwords in real system (i.e., in an environment where the passwords will be used frequently over a period of time). For example, do they contain dictionary words, do users prefer stories while creating passwords, what patterns they exhibit. In short, will they be easy to guess? If answers to most of these questions are affirmative then, our scheme can aid to memory benefits of earlier graphical authentication schemes.

### 6.1 Outline of the user study

We integrated USER AUTHENTICATION BY SECURED GRAPHICAL PASSWORD IMPLEMENTATION with a simple online course management portal. The access to the course content such as lecture notes, weekly exercise etc. was protected with USER AUTHENTICATION BY SECURED GRAPHICAL PASSWORD IMPLEMENTATION authentication scheme. The user study was conducted in the fall semester of 2009 in a second year computer Science Engineering university class, over a month's period, from late November to late December. In total 35 subjects participated, including 32 undergraduate students, 2 graduate students (Teaching

Assistants) and 1 professor. Twenty-five participants are male and 10 participants are female; the ages range from 20 to 45 with average of 22. The participants were from different regions of India, so apparently our participants represent a multicultural community.

At the start of the study, participants were given a 15-minute tutorial in the class by the first author of this paper. Because our user group consists of experienced computer users with solid computer knowledge and represents a relatively high education level, they might perform better than the general population in understanding our scheme. To somewhat compensate for this, we only used plain language in the tutorial (no technical terms were mentioned, such as mapping of pictures to passwords or how a password is encoded). We estimate the attendance rate on the day of the tutorial was approximately 85%. Our password scheme was then explained. Students were not given suggestions about how to choose a secure password or use any mnemonic strategy. A FAQ page was made available on the website in case they need help.

## 7. CONCLUSION

In this paper, we have presented USER AUTHENTICATION BY SECURED GRAPHICAL PASSWORD IMPLEMENTATION, a Secure graphical authentication scheme, strong enough for banking, finance ,e-commerce and sensitive organization. Its strength lies in its simplicity and unique graphical way of working. We have designed and secure prototype of USER AUTHENTICATION BY SECURED GRAPHICAL PASSWORD IMPLEMENTATION. We discussed possible attacks on our scheme and how we could defend each of them. Results of the user study provide evidences for improved usability and memorability. Our future work includes working on the feedbacks received by the participants (using personal pictures and improving the visual search) and testing the scheme with large audience of all ages and under secure password inferences.

## 8. ACKNOWLEDGMENTS

We would like to thank anonymous reviewers for their valuable comments. We also thank mu guide and my friend and the participants from the user study for their support and early feedbacks on the design. We also sincerely thank the members of Internet Picture Dictionary group for allowing us to use their images in the prototype design.

## 9. REFERENCES

- [1] Chiasson, S. Usable Authentication and Click based Graphical passwords. Phd Thesis, Carlton University, Ottawa, Canada. Jan. 2009 .
- [2] Cranor, L., and Garfinkel, S. 2005. Security and Usability: Designing Systems that People can use. O'reilly Media.
- [3] Wiedenbeck, S., Waters, J., Birget, J., Brodskiy, A., and Memon, N. 2005. PassPoints: design and longitudinal evaluation of a graphical password system. *Int. J. Hum.- Comput. Stud.* 63, 1-2 (Jul. 2005), 102-127.
- [4] Feldmeier, D. C., and Karn, P. R. 1990. UNIX Password Security - Ten Years Later. In *Proceedings of the 9th Annual international Cryptology Conference on Advances in Cryptology (1989)*. 44-63.
- [5] Nelson, D. L., Reed, U. S., & Walling, J. R. (1976). Pictorial superiority effect. *Journal of Experimental Psychology: Human Learning & Memory*, 2, 523-528.
- [6] Standing, L. Learning 10,000 pictures. *Quarterly Journal of Experimental Psychology* 25 (1973), 207-222.
- [7] Davis, D., Monrose, F., and Reiter, M. K. 2004. On user choice in graphical password schemes. In *Proceedings of the 13th Conference on USENIX Security Symposium - Volume 13 (2004)*. 11-11.
- [8] Shepard, R. Recognition memory for words, sentences, and pictures. *Journal of Verbal Learning & Verbal Behavior*. 6(1967), 156-163.

- [9] Nali, D., and Thorpe, J. Analyzing user choice in graphical passwords. Technical report, TR-04-01, School of Computer Science, Carleton University, May 2004.
- [10] Jermyn, I., Mayer, A., Monrose, F., Reiter, M. K., and Rubin, A. D. 1999. The design and analysis of graphical passwords. In Proceedings of the 8th Conference on USENIX Security Symposium. 8(1999). 1-1.
- [11] Wiedenbeck, S., Waters, J., Birget, J., Brodskiy, A., and Memon, N. 2005. PassPoints: design and longitudinal evaluation of a graphical password system. *Int. J. Hum.- Comput. Stud.* 63, 1-2 (Jul. 2005), 102-127.
- [12] Khot R. A., Srinathan K., Kumaraguru, P. Marasim: A Novel Jigsaw Based Authentication Scheme using Tagging , To appear, In the Proceedings of 29th Conference on Human Factors in Computing systems (CHI 2011). ACM.
- [13] Jermyn, I., Mayer, A., Monrose, F., Reiter, M. K., and Rubin, A. D. 1999. The design and analysis of graphical passwords. In Proceedings of the 8th Conference on USENIX Security Symposium. 8(1999). 1-1.
- [14] Dirik, A. E., Memon, N., and Birget, J. 2007. Modeling user choice in the PassPoints graphical password scheme. In Proceedings of the 3rd Symposium on Usable Privacy and Security (2007). SOUPS '07, 20-28.
- [15] Renaud, K. and De Angeli, A. 2009. Visual passwords: cure- all or snake-oil? *Commun. ACM* 52, 12 (Dec. 2009), 135-140.
- [16] Davis, D., Monrose, F., and Reiter, M. K. 2004. On user choice in graphical password schemes. In Proceedings of the 13th Conference on USENIX Security Symposium - Volume 13 (2004). 11-11.
- [17] Goldwasser, S., Micali, S., and Rackoff, C. 1985. The knowledge complexity of interactive proof-systems. In Proceedings of the seventeenth annual ACM symposium on
- [18] Bedworth M. A. Theory of Probabilistic One-Time Passwords, [http://www.pinoptic.com/downloads/wp002\\_a\\_theory\\_of\\_potp.pdf](http://www.pinoptic.com/downloads/wp002_a_theory_of_potp.pdf)
- [19] Brostoff, S., and Sasse, M.A. Are Passfaces more usable than passwords? A field trial investigation. Proceedings of HCI on people and Computers XIV, (HCI 2000), 405-424.

# Embedded Based Real-Time Monitoring and Controlling System for Fish Hatchery

Aji Joy

Assistant Professor, Electronics and Communication Engineering Department  
Mar Athanasius College of Engineering, Kothamangalam, Kerala, India. Email : ajijoy@mace.ac.in

**Abstract**—In this paper a real time monitoring and controlling system for Fish hatchery is designed, developed and proposed. The pH, dissolved oxygen, salinity, temperature and water level are prominent parameters which are responsible for the sustained growth of fishes. Mainly hatcheries of fresh water ornamental fishes are concentrated. Dissolved Oxygen content is a highly important parameter which if not available in the required amount will affect the growth of fishes and even lead to death. Salt helps in fighting disease, parasites and chemical poisoning. The pH is a key parameter that has to be maintained between 6.0 and 8.0. Temperature is in turn another important parameter which affects the health of fishes as well as the pH value. The proposed system monitors and controls the above said parameters. A real time video streaming unit is also incorporated into the system in order to have round the clock surveillance of the farm. Web server is designed to host a portal and help the person in charge to monitor the farm remotely.

**Keywords-** pH, Dissolved Oxygen, Salinity, Temperature, Water level, Portal, Web server.

## I. INTRODUCTION

A fish hatchery is a facility designed to raise fish. It provides an optimum environment for fish to grow by maintaining proper pH value, salinity, water temperature, oxygen levels, safety etc. In order to survive in fresh water, the fish needs a wide range of physiological adaptation in order to keep the ion concentration in their body balanced. Fresh water fishes require a salinity level 0-0.05%. The pH is a key parameter which affects the life of fishes and is best between pH 7.0 to 8.0. Fresh water has a natural pH range of 6.0 to 8.0. The small changes in the value of pH make the life of fish highly stressful and toxic. Temperature is another key parameter that influences the value of pH. At elevated temperatures the toxicity level increases which affect the fishes. Salt being a natural ingredient make the fishes feel home and defeats toxic chemicals and avoid fish poisoning. It also helps to gain energy due to illness and stress and hence helps in their metabolism. In an aquarium like atmosphere the density of fishes is very high. The dissolved oxygen content can be very easily go down and it makes a hazardous situation. The water has to be aerated to top-up the oxygen levels. One approach to resolve all the above problems is to employ a sensor circuit which monitors the required parameters such as pH, dissolved oxygen, temperature, salinity and water level.

TABLE I  
WATER QUALITY PARAMETERS AND THEIR STANDARD VALUES

SI No	Parameter	Standard values	
1	Dissolved Oxygen	>4.0 mg/l	
2	Temperature	Species Dependent	
3	pH	7.5-8.5	
4	Salinity	Freshwater	<0.5 ppt
		Brackishwater	0.5-30 ppt
		Seawater	30-40 ppt
		Brine	>40ppt
5	Carbon dioxide (CO <sub>2</sub> )	<10 ppm	
6	Ammonia (NH <sub>4</sub> <sup>+</sup> /NH <sub>4</sub> N)	0-0.5 ppm	
7	Nitride(NO <sub>2</sub> )	<1 ppm	
8	Hardness	40-400 ppm	
9	Alkalinity	50-300 ppm	
10	H <sub>2</sub> S	0 ppm	

## II. PROPOSED SYSTEM

In the proposed system an AVR microcontroller is used for real time analysis, monitoring and controlling of the different conditions. A pH meter is calibrated to sense the value of pH of the fresh water, and when it

exceeds, alkaline solution is poured in using a pump to maintain the required value of pH for water. A temperature sensor LM35 attached to the system senses the variations in water temperature and whenever the temperature exceeds the critical values, cooling system or heating system is activated in accordance to it. When the oxygen level goes below the critical value due to the high population density of the fishes the Aerator is activated to bring it back to the optimum condition. There is a water level sensing unit and using water pumps the water level is also maintained. Alarm goes on for conditions exceeding the optimum threshold levels. An alert message and the current parameter values are sending to the concerned persons mobile as well as to the system via GSM module, to inform the present status. For real time monitoring of the conditions, there is a wireless web cam which is used to stream real time video to the control room. The received values at the system are sending to a portal, so that the values can be monitored via internet.

### III. HARDWARE DESCRIPTION

The monitoring system consists of Atmega32 microcontroller and a set of sensors. Figure 1 is the block schematic and Figure 2 is the circuit diagram of the system. In order to monitor the different parameters we make use of corresponding sensor units.

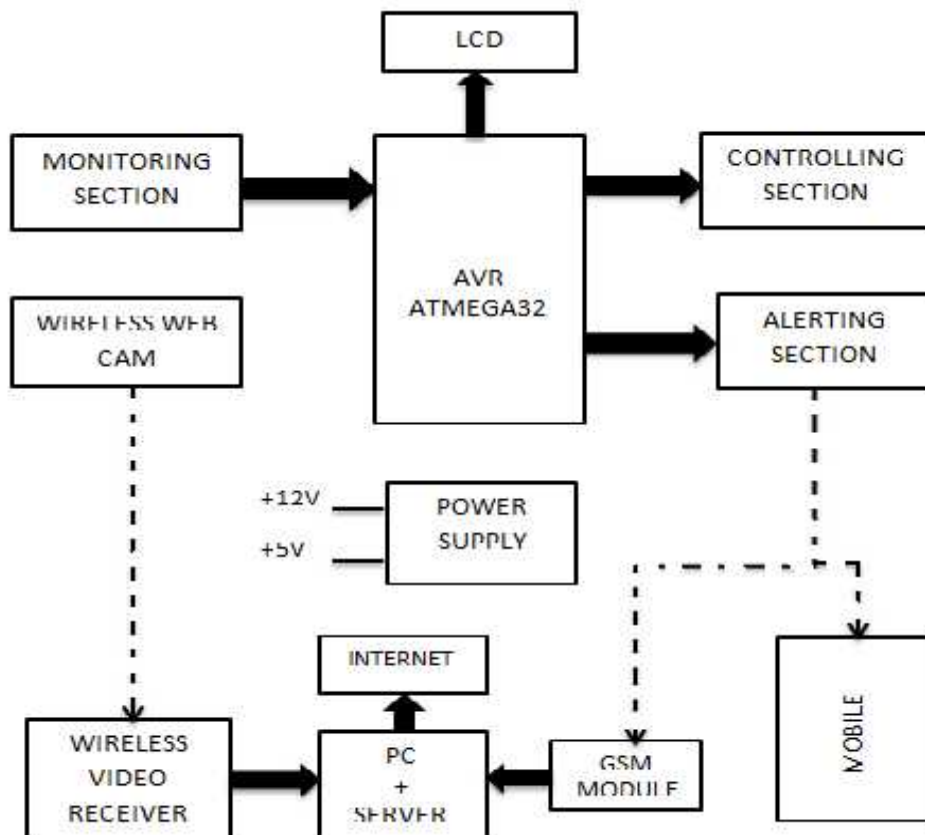


Figure 1. Block Diagram for the monitoring of fish hatchery.

Each parameter is monitored continuously using different types of sensors and analysed the values for the requirement of control over the parameters. When the monitored value exceeds the critical limits, the controlling section comes into action and brings back the optimum condition. An alert message also will be sent from the control unit. The user is also updated with the scenario of the hatchery with the help of 24 hour video streaming, so that they can avoid intruders. For real time surveillance, even if the user is far away from the hatchery, can get the updates and monitored values and details of the hatchery, with the help of Internet. For that a portal is created, which gives the updated information.

#### A. Monitoring Sections

1) *pH*: In this project a glass type combination electrode type pH sensor is used. In that type the measuring and reference electrodes are joined together in a single glass body assembly. The pH measurement is comprised of two half-cells, or electrodes. One half-cell is the pH sensitive glass measuring electrode and the other is the

reference electrode. Just as the two half-cell potentials of a battery are required to complete a circuit so does a pH sensor. It uses a potentiometric measurement technique. The mathematical expression for this is:

$$E = E_m - E_r$$

Where,

E=Potential developed at the electrode output

$E_m$  = the electrode potential of the measuring electrode

$E_r$  = the electrode potential of the reference electrode

Combined pH electrode is used to measure the value of pH which is a kind of immersion probe with a precision of  $\pm 0.01\%$ . It gives an output range of 4 to 10. As the optimum range for fresh water fishes is 6.0 to 8.0, if the value drop is below 7.0, a pumping system is activated to pump in alkaline solution and thus brings back the optimum condition. The analog output obtained is given to the ADC pins of the AVR and the corresponding digital output is obtained. The range of pH required varies with fishes.

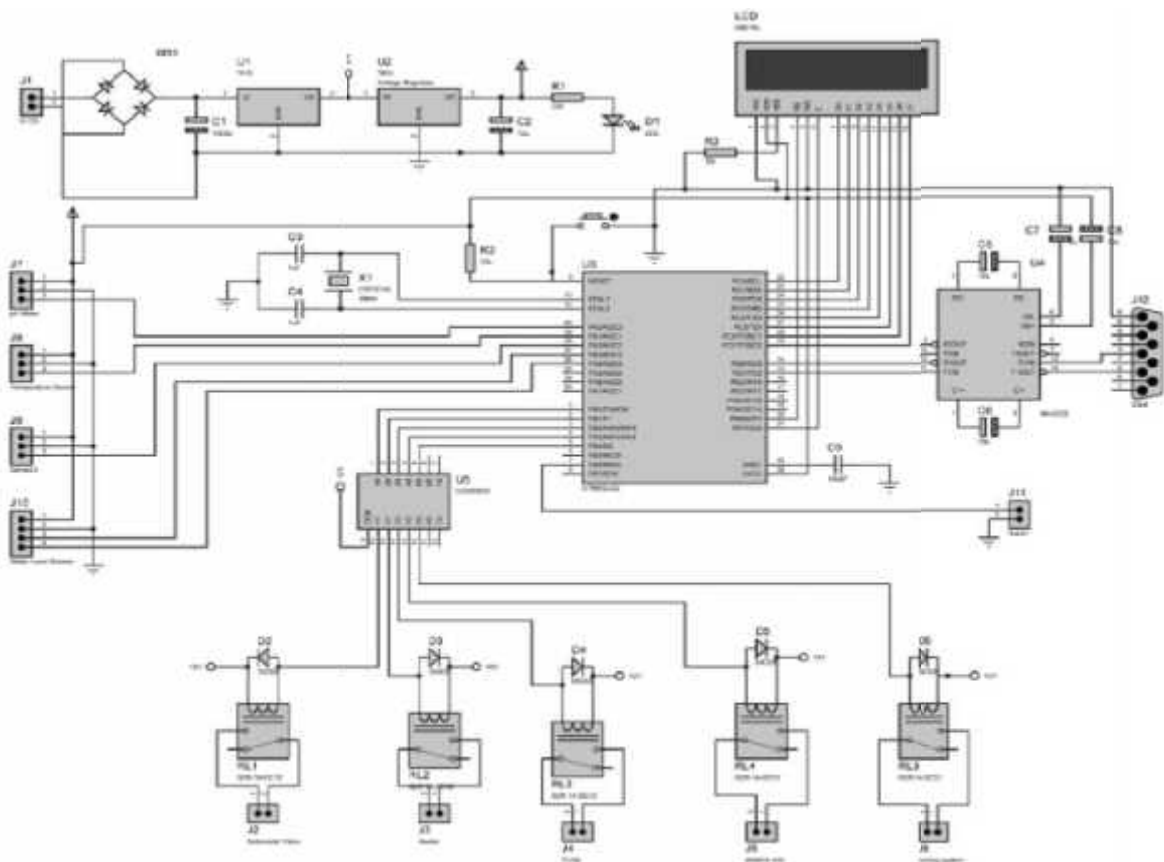


Figure 2. Circuit Diagram for the monitoring and control system of fish hatchery.

2) *Dissolved Oxygen*: To keep the water with saturated oxygen the water will be sprinkled through fresh air as fine particles and the water will be saturated. Additional aerator is also provided in the fish tanks for the additional supply of oxygen to the water.

3) *Salinity*: Salinity is the amount of dissolved salt in water. For fresh water fishes a range of 0-5 grams of salt per 1 kl of water is considered to be safe. Depends on the species of the fish an optimum value will be set. Salinity meter is used to check the salt content in water and the lower threshold level is set as 0.3ppt. If it goes below this, rock salt is pumped into water and thus optimum condition is maintained. Even if the fresh water is free from salt, to keep a better atmosphere for fish by keeping away the diseases, parasites and toxic items adding salt is a must.

4) *Temperature:* Temperature sensor LM35 produces an analog output with change in temperature which is about 10 mV per degree. The output of the temperature sensor is connected to the ADC pin of the AVR which gives a digital output which is then converted to degrees with the help of software. The lower and upper threshold is set as 20 and 30 degree Celsius respectively, as it is the optimum range for ornamental fishes. Fresh water is circulated to cool off the water and heater is switched on to heat the water up.

5) *Water level:* For different fish species, the depth of water they resides varies. So, water level too is an important factor in fish farming. In order to detect the water level, we make use of a variable resistance float type sensor. In which the resistance will changes with variation in water level.

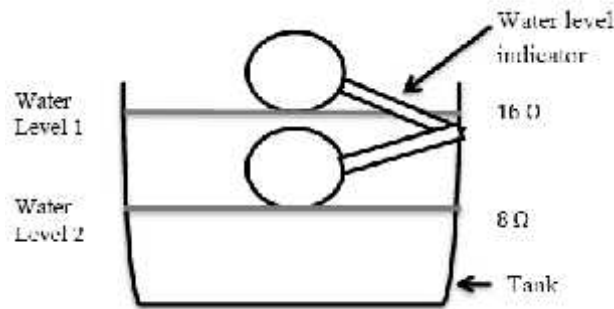


Figure 3. The float mechanism to sense the water level.

The above figure shows how the water level indicator used in this project works. As it is a float type, it floats on the surface of the water. It moves up and down corresponding to the increase and decrease of the water level. Resistance values for two levels (level 1 and 2) are shown above. The output of this indicator is given to two ADC input pins of the AVR.

### B. Controlling Sections

1) *Alerting Unit:* The main parts of the alerting unit are a buzzer and a GSM modem. The buzzer goes on for few seconds to alarm the person in the control room or in the vicinity of the system that one of the monitoring parameter has exceeded the critical value. The GSM modem is used to send alert and other messages to the concerned person. When a request is made via the web page to read a particular parameter value, the value will be read from the portal. The portal is updated at regular intervals or on demand.

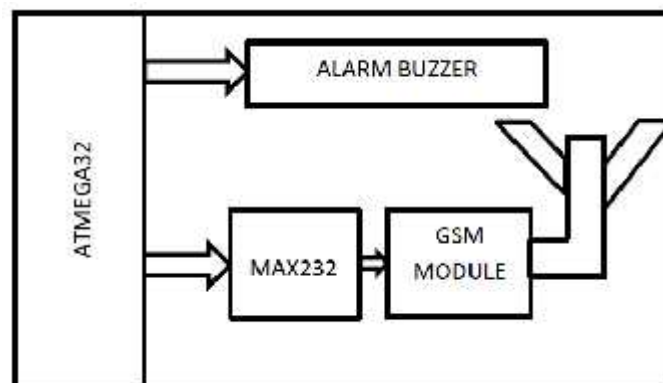


Figure 4. The Alerting Unit of the System.

2) *Controlling Unit:* The threshold values of each parameter is checked continuously, when this exceeds a threshold critical value the alarm buzzer goes on, and a message is send to the user indicating the change in the parameter value, along with all this these parametric values can be viewed by the user through the web page provided, the current value and the history of values recorded with the help of the web server. This page can be accessed by the user from anywhere around the world via internet.

3) *Real Time Monitoring and Operation:* The wireless web cam connected in the system streams a real time view of the surroundings of the hatchery round the clock to the control room. The video sent are of 2.4 GHz RF to the wireless video receiver connected to a PC in the control room. The received video is thus viewed here using the software called as Honestech2.5 and any abnormalities or extra presence of weird things is identified. This software has the options to play, pause, re-play, rewind, stop etc., so that the video can be viewed conveniently according to the user's need and time.

The web server designed is used to store the values of the monitored parameters in a database. A web page is exclusively designed for this project via Adobe Dreamweaver and Netbeans software. Html language to used to design and set the web page. Java is incorporated into this system to access the received parameter values via the serial port (GSM module unit) and store it in the database.

Initially a request is made from the embedded section to help understand the java section about the GSM number. Once the request is made, the GSM number in the embedded section is extracted and stored for further communication. Then at each time the user requests the parameter values via a java application, it is send via GSM to the embedded unit, and the values are received in a specific format and are stored in a database. This message is received and processed at the destination and is understood that the pH value is been requested. Hence the pH value, the value is sent in this specific format. The received value is inserted into database tables and is uploaded to the web page .The user can hence view the received parameter value in the web site.

Jsp language is used to convert the html codes of the page to create each page in the web site. A user interactive section also provided in the web site so that feedback about this system can send.

#### IV. SYSTEM OVERVIEW

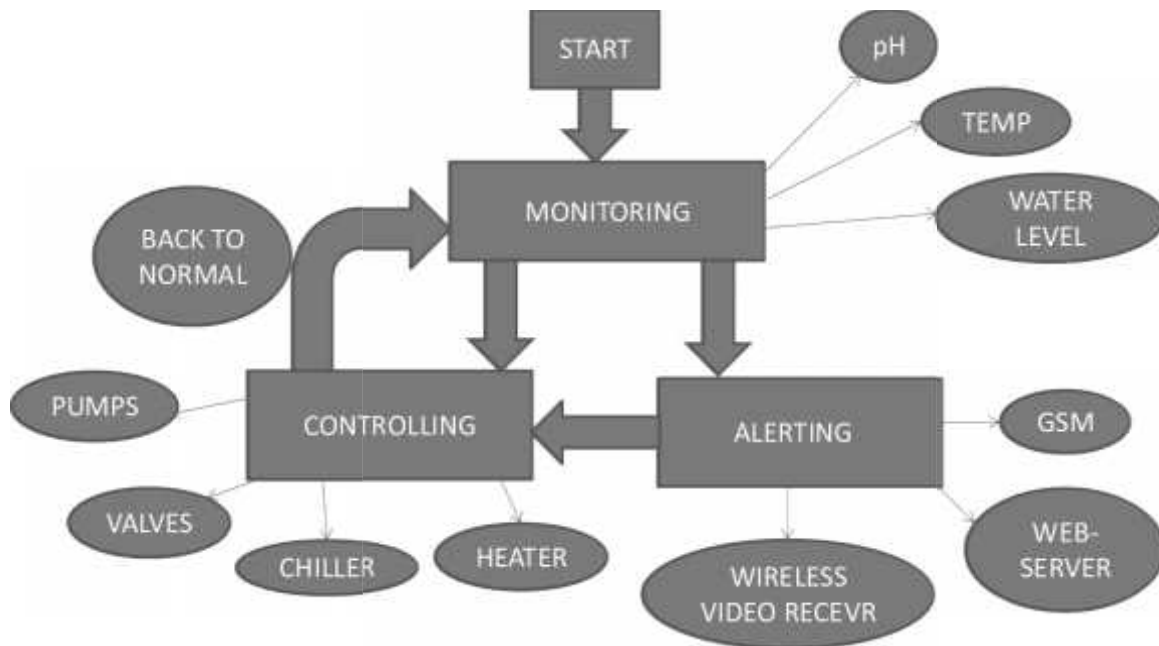


Figure 5. System Overview.

#### V. RESULTS

TABLE III  
MONITORING OF IMPORTANT WATER QUALITY PARAMETERS

SI No	Parameter	Standard values	Values changed by Action	Values corrected by control unit
1	Dissolved Oxygen	>4.0 mg/l	Decreased due high population density of fishes	Corrected by aerator activation
2	Temperature	Species Dependent	Increase/Decrease	Fresh water flow/Heater operation
3	pH	7.5-8.5	Increased by Temperature increase	Corrected by Alkaline pump
4	Salinity	<0.5 ppt	Fresh water salinity is naturally low	Increased to 0.3ppt by addition of brine for healthy surroundings for the fish.

Most of the critical factors which can affect the life of fish in a hatchery are identified and monitored in real time. Many of the parameters are controlled automatically without the intervention of human being. By this the volume of production can be improved and the cost can be reduced.

## VI. CONCLUSION

The developed prototype can control the real time hatchery environmental factors such as pH, dissolved oxygen, salinity, temperature and water level. It has proven to successfully acquire accurate measurements for the above said parameters. The alarming message is sent to the user if the value monitored is more or less than the upper and lower threshold values respectively. So this helps us to monitor the fish hatchery and facilitate the stay of fresh water fishes comfortably. In future, the alerting system can be extended to applications of very long distances.

In this project, using AVR microcontroller for real time analysis and monitoring of pH, water level and temperature, we provide optimum conditions for the growth of ornamental fishes. Alarms are set for every system which goes on for conditions exceeding the optimum levels; also an alert message is sent to the concerned persons mobile via GSM module, to alarm the person about the present situation of the hatchery. A wireless web cam is used to stream real time video to the control room (PC) through wireless video receiver.

We have also implemented a website along with this project to make it more flexible and easy monitoring. Through this project, we can automatically monitor and control the water parameters. It's very easy to install and maintain.

## REFERENCES

- [1] M.Lopez, J.M. Gómez, J. Sabater, A. Herms, "IEEE 802.15.4 based Wireless monitoring of pH and temperature in a fish farm," IEEE 2010 Conference.
- [2] Santoshkumar et al. "Design and Development of Wireless Sensor Network System to Monitor Parameters Influencing Freshwater Fishes," International Journal on Computer Science and Engineering (IJCSSE), Vol. 4 No. 06 June 2012.
- [3] Bodepudi SrinivasaRao, U.Jyothi Kameswari, "Design an Monitoring System of Aquaculture with Multi-Environmental Factors Using ARM7," International Journal of Computer Science and Information Technologies, Vol. 3 (3) , 2012,4079-4083.
- [4] Edthofer, F, Van den Broeke, J., Ettl, J. , Lettl, W, " Reliable online water quality monitoring as basis for fault tolerant control," IEEE Conference on Control and Fault-Tolerant Systems (SysTol), 2010.
- [5] Hashemian, H.M., "Applying Online Monitoring for Nuclear Power Plant Instrumentation and Control," Nuclear Science, IEEE Transactions on (Volume:57 , Issue: 5 ).
- [6] Chen, Y.C., "Pressure control through online monitoring ," IEE Colloquium on Control and Optimisation Techniques for the Water Industry, 9 May 1990.
- [7] Changyong Zhang, "Design of monitoring and controlling system for airfield lighting based on computer," 8th World Congress on Intelligent Control and Automation (WCICA), 2010.

## BIOGRAPHY



**Aji Joy** received his B. E. degree in Electronics and Communication Engineering from Mangalore University, Karnataka, India in 1996 and the M. E. degree in Power Electronics and Drives from PSG College of Technology, Tamil Nadu, India in 2008. Currently he is carrying out research at the PSG College of Technology, Tamil Nadu, India. His main interests lie in the architecture of Open CNC, PLC, and Embedded systems. He is working as Assistant Professor in the Department Electronics and Communication Engineering, Mar Athanasius College of Engineering, Kothamangalam, Kerala, India.